

University of Texas Rio Grande Valley

ScholarWorks @ UTRGV

Theses and Dissertations

12-2016

Wettability of nonwoven polymeric nanofiber mats

Edgar Munoz

The University of Texas Rio Grande Valley

Follow this and additional works at: <https://scholarworks.utrgv.edu/etd>



Part of the [Mechanical Engineering Commons](#)

Recommended Citation

Munoz, Edgar, "Wettability of nonwoven polymeric nanofiber mats" (2016). *Theses and Dissertations*. 194.
<https://scholarworks.utrgv.edu/etd/194>

This Thesis is brought to you for free and open access by ScholarWorks @ UTRGV. It has been accepted for inclusion in Theses and Dissertations by an authorized administrator of ScholarWorks @ UTRGV. For more information, please contact justin.white@utrgv.edu, william.flores01@utrgv.edu.

WETTABILITY OF NONWOVEN POLYMERIC NANOFIBER MATS

A Thesis

by

EDGAR MUNOZ

Submitted to the Graduate College of
The University of Texas Rio Grande Valley
In partial fulfillment of the requirements for the degree of

MASTER OF SCIENCE ENGINEERING

December 2016

Major Subject: Mechanical Engineering

WETTABILITY OF NONWOVEN POLYMERIC NANOFIBER MATS

A Thesis
by
EDGAR MUNOZ

COMMITTEE MEMBERS

Dr. Karen Lozano
Chair of Committee

Dr. Horacio Vasquez
Committee Member

Dr. Rogelio Benitez
Committee Member

Dr. Mataz Alcoutlabi
Committee Member

December 2016

Copyright 2016 Edgar Muñoz

All Rights Reserved

ABSTRACT

Muñoz, Edgar, Wettability of Nonwoven Polymeric Nanofiber Mats. Master of Science Engineering (MSE), December, 2016, 62 pp., 4 tables, 18 figures, references, 48 titles.

The wettability of heterogeneous materials has been attracting special interest by academia and industrial sector given the need to development self-cleaning Nonwoven nanofiber mats have demonstrated potential given its hydrophobicity granted by the ultimate structure of the system, small fiber diameter and small pores giving rise to effects such as the Cassie-Baxter. This thesis analyzed the wettability of a wide range of polymeric systems. Nanofiber mats were manufactured using the Forcespinning® technology. Samples were prepared at different polymeric concentrations and rotational speeds to alter fiber size; density of the mat was also altered to evaluate the effect of porosity on the wettability. Scanning Electron Microscopy (SEM) was used to characterize the mats and contact angle studies were conducted to better understand wettability of the developed surfaces.

DEDICATION

The completion of this Thesis studies would not have been possible without the love and help of the Holy Spirit and support of my family, my mother, my father, sisters, and lovely nephews. All these individuals helped me in the completion of this project and encouraged me to accomplish this degree. Thank you for your patience, love and the way of pushing me to achieve my goals. There is always a light at the end of the tunnel, there is always a positive impact after rough situations in life.

ACKNOWLEDGEMENTS

I will always be grateful to Dr. Karen Lozano, chair of my Thesis committee, for her friendship, mentoring and advice. From the introduction into the polymer world and nanotechnology the idea for this Thesis research in the wettability analysis of fiber materials. She always encouraged me to complete my Thesis and she devoted much time and effort to guide me through the process. Many thanks go to my Thesis committee members: Dr. Horacio Vasquez, Dr. Rogelio Benitez, and Dr. Mataz Alcoutlabi. Their advice, input, and observations on my Thesis helped to ensure the quality of my intellectual work. I would also like to thank my colleagues and friends at the UTRGV mechanical engineering department who facilitated the use of the imaging tools required to characterize my samples, Hilario Cortez. This project is supported by NSF PREM award under grant No. DMR-1523577: UTRGV-UMN Partnership for Fostering Innovation by Bridging Excellence in Research and Student Success

TABLE OF CONTENTS

	Page
ABSTRACT.....	iii
DEDICATION	iv
ACKNOWLEDGEMENTS	v
TABLE OF CONTENTS.....	vi
LIST OF TABLES	viii
LIST OF FIGURES	ix
CHAPTER I. INTRODUCTION.....	1
CHAPTER II. LITERATURE REVIEW	3
2.1 Consequences of Biofouling	4
2.2 Methods of Antifouling.....	5
2.3 Biological Effects of Biofouling	7
2.4 Ice Formation on Solid Surfaces	8
2.5 Cassie-Baxter Effect.....	10
2.6 Polymeric Nano-micro Fibers	17
CHAPTER III. EXPERIMENTAL PROCEDURE.....	26
3.1 Forcespinning Technology	27
3.2 Contact Angle	27
3.3 Scanning Electron Microscope.....	29
3.4 Manufacturing Parameters	32

3.4.1 Polymeric Solution Concentration	33
3.4.2 Rotational Speed	33
3.4.3 Distance from Collector System to Spinneret	34
3.5 Contact Angle Meter	34
CHAPTER IV. EXPERIMENTAL SET UP	36
4.1 Polymeric Solution Preparation	36
4.2 Fiber Fabrication	36
4.3 Fiber Collection	37
4.4 Scanning Electron Microscope.....	38
4.5 Contact Angle Measurements	38
4.6 Evaluation of Algae Attachment	42
CHAPTER V. RESULTS AND DISCUSSION	45
5.1 Morphology of Nonwoven Polymeric Nanofiber Mats	45
5.2 Contact Angle of Nonwoven Polymeric Nanofiber Mats	46
5.3 Work of Adhesion of Nonwoven Polymeric Nanofiber Mats.....	51
CHAPTER VI. CONCLUSION	55
CHAPTER VII. FUTURE APPLICATIONS	56
REFERENCES	58
BIOGRAPHICAL SKETCH	62

LIST OF TABLES

	Page
Table 1. Density and Surface Tension of Probe Liquids at certain Temperature	42
Table 2. Contact angles and Work of adhesion of Bulk and Fibers for Nylon6.....	51
Table 3. Contact angles and Work of adhesion of Bulk and Fiber mats for PVDF.....	53
Table 4. Contact angles and Work of adhesion for Bulk and Fiber mats for Various Polymer. ..	53

LIST OF FIGURES

	Page
Figure 1. Cassie-Baxter Effect	12
Figure 2. Unequal forces experienced by molecules at the surface of the liquid.	14
Figure 3. Intermolecular interaction of Liquid and Surface	15
Figure 4. Contact Angle	28
Figure 5. Scanning Electron Microscope	29
Figure 6. Simplified Diagram of SEM (prehistoric-colours-blog)	32
Figure 7. A) Fiber collection system, B) Collector and C) Fiber mat	37
Figure 8. Sputtering Fibrous Materials	38
Figure 9. A) Contact angle meter and B) Fiber mat	39
Figure 10. Points of selection for Contact Angle.....	40
Figure 11. LBADSA	40
Figure 12. Probe Liquids.....	42
Figure 13. Naturally collected Algae	43
Figure 14. Culture of Algae in different mediums.....	43
Figure 15. Algae study with PTFE and PP	43
Figure 16. 3D Random distribution nonwoven mat.....	47
Figure 17. SEM Images of various fiber mats fabricated by Forcespinning	51
Figure 18. Schematic Illustrating the sagging of liquid on the fiber surface.	54

CHAPTER I

INTRODUCTION

The wetting of surfaces has been an area of interest for several decades, though the interest has recently intensified given the proliferation of nanofibers and ability to tailor surfaces at the nanoscale. Academia and industry are actively searching for new materials or methods to develop surfaces with controlled micro-nano structures to effectively control the ability of attract or repel water and/or other liquids from its surface. Morphology and chemical composition are the main characteristics that control the wettability of a surface. Most of the technology development in this area have been inspired by self-cleaning surfaces from nature such as the *Lotus leaf*. Cassie-Baxter model, predicts that the surface roughness can easily change the water Contact Angle (CA) over 150° (superhydrophobic) to 0° (superhydrophilic). This thesis focuses on wettability studies of heterogeneous surfaces obtained from nonwoven polymeric nanofiber mats. Chapter 2 elucidates the current state of the art; an extensive literature research was conducted and summarized in this chapter. Current applications and state of the art development of rough surfaces are explained as well as testing procedures and theories. Chapter 3 describes the different experimental techniques and testing procedures specifically used in this study. Chapter 4 describes the experimental steps followed to complete the study. Starting from the preparation of polymeric solutions, experimental parameters used for developing the nonwoven nanofiber mats and preparation of sample for different testing methods such as scanning electron microscope (SEM) and CA measurements.

Chapter 5 presents the results CA and work of adhesion as well as in-depth discussion of the relationship between fiber diameter, porosity, and thickness of the mats. Chapter 6 concludes the study points out learned lessons. Chapter 7 presents new directions and potential applications of the analyzed surfaces.

CHAPTER II

LITERATURE REVIEW

Industry and scientific communities had given great attention to surfaces with a unique wettability phenomenon. The wetting of solids by liquids can be determined quantitatively by the values of contact angle CA. Wettability studies are considered fundamental to understand the physical-chemical interactions of surfaces in contact with water or in aqueous environment [1]. Superhydrophobic surfaces can be accomplished by a combination of appropriate roughness and low surface free energy. Surface roughness has been shown to play a key role in a wide range of practical applications such as self-cleaning, ice-phobic, antifouling, inkjet printing applications and biofluidic manipulation [2].

Naval and Marine industries have been facing corrosion problems on the hull of ships due to fouling (attachment of microorganisms to surfaces of bodies submerged or in contact with the flow of water). Specifically, fouling occurs given the settlement and growth of plants and animals such as bacteria, fungi, algae, and barnacles that produces a layer of slime on the contact surface. Aesthetically, in the naval industry, it presents a problem but it is much more than that, fouling interferes with the mechanical efficiency of the ships and with that lifetime of the components, it highly promotes corrosion. More than 4,000 organisms exist in the marine environment and range in size from micrometers (bacteria, algae spores) to centimeters (barnacles, oysters, mussels) [3]. The way organisms attach to the surface varies according to each organism. Several organisms

attach temporarily to one surface but later reattach to another surface permanently. A common type of marine organism is the microalgae, *Ulva*, which attaches poorly to a surface while looking for an active surface to attach permanently. The attachment of bacteria on the surface results in the production of a biofilm that initiates or accelerates the electrochemical process of corrosion. The formation of the biofilm is the beginning of the colonization of different microorganisms such as barnacles, algae, protozoa and fungi. The process is initiated by electro kinetic interactions between the surface and organisms followed by their attachment and growth. Bacterial adhesion, growth, and proliferation resulting a generation of slime beginning to shelter other organisms. Extreme fouling results in high concentration of masses, which eliminate the smoothness of the surface and alter the shape of the hull; therefore, creating large dragging forces that interfere with the speed throughout motion. Forces created by the dynamics of fluids are the major mechanisms of transportation of microorganisms. Structures, ships and membranes are the most predominant surfaces of fouling due to their contact with forces of water.

2.1 Consequences of Biofouling

The process of metals deteriorated by microorganisms such as bacteria, is called microbiologically induced corrosion (MIC). Bacteria create sulfides and results in pitting and corrosion at the surface. Bacteria can be aerobic (requires oxygen to survive) or anaerobic (does not requires oxygen to survive). Aerobic bacteria are mostly present in the marine environment. The MIC corrosion imitates when bacteria seeks out metal surfaces such as carbon steels, stainless steel, aluminum, and copper alloys to sit on their surfaces producing a degradation by the interactions of the surface with bacteria waste. The interactions between the surface and organisms can be minimized by reducing the surface and interfacial energies. If the problem is detected on time and proper maintenance is offered, the lifetime of the ship (given corrosion induced problems) can

increase up to 20%. The key to reducing fouling on ship surfaces is to apply a fouling inhibitor this will reduce the attachment of organisms that forms in part by the MIC corrosion process. The development of hydrophobic and superhydrophobic surfaces is key to reduce the growth and attachment of organisms, these are called anti-corrosive and antifouling surfaces. Hydrophobic surfaces provide low energy at the surface minimizing the interactions between the atoms from the surface and molecules from the environment. The differences of attachment and settlement among organisms is difficult to predict and understand. The wettability of each organism is critical since each organism seeks for a surface with the same wettability. New knowledge in how organisms attach, grow and proliferate has ignited the development of new materials which have tailored surfaces to improve anti-fouling properties.

2.2 Methods of Antifouling

Copper biocides paints are among the most used fouling inhibitors [4]; however, these paints pose an environmental issue and can be hazardous to marine animals. Alternative fouling inhibitors have been developed throughout the years although most still contain metals such as copper. Foul release coatings (FRC's) are an alternative way to control fouling. The development of new antifouling inhibitors is expected to save over 150 billion per year [3]. Coatings must perform in several extreme environments such as different temperature, pH, salinity, and flow rates. The alkalinity of the marine environment, measured by pH, can alter the corrosion process. An acidic marine environment, or low pH, enhances the corrosion process. Another factor to consider in the process is that the exposed surface can contain charged particles or components that when opposite charges are encountered, electrostatic charges in between the surface and the environment can ignite the fouling process.

On the other hand, if the environment and surface substrate have the same charges they will repel each other and the possibility of fouling will be eliminated. Zwitterionic materials provide garnered attention since these materials contain anions and cations. The anions are in one side while the cations are on the other side. Once these ions attract one another they will neutralize the surface and the material will no longer be charged. Charge neutrality of the surface will cancel the attraction due to electrostatic nature though still fouling could occur through other processes. The types of forces involved in adsorption include Van der Waal's and electrostatic interactions [5]. Additionally, organisms with flagella can propel or move themselves in water and then attach to the surface. The adhesion forces contribute to the surface tension between the organism and surface. Roughness is another factor that contributes to colonization by sheltering organisms in the grooves generated by roughness. The preparation of zwitterionic materials requires several steps in which a polymeric material is modified [6]. One such approach to fabricating an antifouling material is to develop a hydration surface, whereby water molecules within the polymer chain contain high specific adsorption of proteins [7]. The hydration surface must be directly related to the environment with the specific organism.

It has been determined that a key parameter to the development of an antifouling surface is to increase its hydrophobicity. Hydrophobic surfaces contain non-polar groups that preclude the ability to interact with water. Contrary, hydrophilic surfaces contain polar groups that promote wetting the travel of the organism to the surface and therefore initiating an interaction with the environment. In the case of hydrophobic surfaces, organisms cannot adhere to the surface unless an external force is present. [8]

2.3 Biological Effects of Biofouling

Microbiologically induced corrosion (MIC), as described above, is a common type of corrosion that occurs when microbiological organisms attach to the surface producing a metabolic reaction that actively deteriorates the metal surface. MIC has a biological origin, it initiates or accelerates the electrochemical process of corrosion due to sulfides in the waste of bacteria that starts degrading the grain boundaries of the metal. The process involves the transfer of electrons through oxidation (anode) and reduction (cathode) process. pH and temperature has a strong influence in the rate of transfer (e.g. fast or slow) of microorganisms-surface reaction. The concentration of oxygen at the surface has an important impact in the corrosion process caused by the fouling of microorganisms. Passive films play an important role in the process of corrosion, strong passive films increase protection the metal. In the case of elements such as copper (Cu), the absence of passive film in the bulk produces a secondary process of corrosion due to differences in electronegativity [9].

The first steps of the corrosion process are the formation of a biofilm that is extremely dependent in the environment such as temperature, salinity and pH. Several types of biofilms exist depending on the surrounding environments. Some bacteria can only survive at certain temperatures and salinity. Apart from that, the biofilm acts as an adherent surface for bacteria. Polysaccharides, proteins, lipids, nucleic acids, and microorganisms traps more particles and organisms and adhere it within the biofilm [9]. Sulfuric acid found in marine environments can be metabolized and used by bacteria as a source of food. The biofilm can triggers microorganisms to produce more extracellular polymeric substance (EPS) which further promotes adherence and growth. The settlement of EPS on the surface is called phase 2 formation of biofilm. During phase 3 replications of bacteria occur on the surface over time. Phase 4 is mainly seen when the thickness of the biofilm starts to increase

and more microorganisms become present on the surface. Phase 5 is usually seen when portions of the biofilm are formed away from the hull. The presence of oxides, hydroxides and sulfides mainly produced by bacteria are considered corrosion drivers for MIC, and the main drivers for breaking down the oxide layer. The accumulation of organisms on surfaces in contact with the flow of water, is associated with the fouling increasing fuel consumption due to the increased of the frictional drag. The US Naval Academy has reported that the overall cost associated with the maintenance, coating and cleaning is estimated to be 56 Million per year for the entire DDG-51 fighter class ship [10]. Organisms in water tend to attach/accumulate to bodies in contact with the flow of water. Repelling water molecules from the surface could be a way to prevent organisms in the water to attach to the surface.

2.4 Ice Formation on Solid Surfaces

Morphology and roughness are the main characteristics that determines the fouling of organisms. The attachment of water molecules on surfaces is the very first step of settlement of organisms. Out of water bodies attachment of water molecules on surfaces exposed to freezing temperatures in infrastructures such as wind turbines, power lines and aircraft; results in the formation and accretion of ice producing serious safety and economic problems [11]. Ice adhesion is based on the hydrogen bonding, van der Waals forces, and the electrostatic interactions with the surface. The energy due to the electrostatic interaction between the ice and the metal is higher than van der Waals and chemical bonding interaction.

For scheduled air carriers icing, has been a contributing factor in 9.5 % of fatal air carrier accident. The formation of ice on the surface re-shapes the surface of the lift-producing parts of the airplane changing the aerodynamics of the wing by increasing the resistance force of motion negatively affecting the lift. Typically, ice builds up when tiny cloud droplets impact and freeze on

the leading edges, front surfaces of the plane. The ice on the planes can be formed in two ways: on the ground and on the flight.

On the ground, is just the same as cars left overnight and there is ice formed by the morning time. That type of ice is managed by de-icing the plane with fluid at the airport. In the flight ice formation takes place when the airplane is flying through the clouds made up of small liquid water droplet. It can get down to temperatures of -40°C , even though the freezing temperature of water is 0°C , water stays in liquid form because does not have a surface to freeze.

At the time water impacts the surface of the airplane, it freezes on the frontal surfaces: leading edge of the wings, and empennage surfaces [12].

Ice removal systems such as thermal, mechanical, pneumatic, and chemical have been developed. Mechanical systems are the most effective solutions considering the energy needed and environmentally friendly process and therefore the most used techniques within the aerospace industry [12]. Mechanical techniques consist mainly of breaking the ice by mechanical forces produced by the motion of aircraft components to break the ice. The aircraft components usually by mechanical and hydraulic systems adding more weight to the aircraft. As for thermal systems, ice is eliminated heating specific areas though the water droplets run to unheated and ice is formed.

As for chemical methods, anti-icing is promoted by utilizing glycols to defrost the systems. De-icing fluids such as ethylene and propylene glycols predominantly used for the aerospace industry have high cost and elevated toxicity towards the environment [13]. Eco-friendly solutions are highly desirable. The development of new technologies that decreases or eliminates the formation of ice is an active area of study in several laboratories and national agencies. Studies have shown that superhydrophobic surfaces inspired on nature increased nucleation density; eventually, increasing the condensation of droplets at the surface. The most significant parameters in the

development of ice-phobic surfaces are adhesion strength, energy reduction and microstructural, defects that contribute to the pinning effect, freezing and ice adhesion [11]. The advantage of superhydrophobic surfaces comes mainly from their low surface free energy and low work adhesion; resulting in a low roll-off angle and minimum force to remove the droplet from the surface. Studies had demonstrated that altering the topography of surfaces shear forces such as ~ 40 to ~ 80 kPa required to detach ice from the surface [14]. Several times lower than mirror-polished (~ 360 kPa) and flat fluoropolymer surfaces (~ 190 kPa). Ideal characteristics for the development of surfaces with the ability of repelling water molecules are in current development. In rougher surfaces, the ice formed around the peaks and valleys deforms and breaks, demonstrating that roughness can break the path for fracture propagation and ice adhesion strength [15].

2.5 Cassie-Baxter Effect

In rough heterogeneous surfaces the thermodynamic equilibrium of CA is called the Wenzel and Cassie Baxter model. The Cassie-Baxter effect is based on the ideal wetting behavior for a droplet resting on the peaks of a rougher nano-micro textured surface. Both models depend on the interface of the solid-liquid, generally used to evaluate the CA of superhydrophobic surfaces. Until now, there is not rule or guideline that determines the type of angles according to morphology and chemistry of the surface. Such models of wettability, are increasingly used due to the advances in the development of superhydrophobicity surfaces [16]. Both models work under rough/heterogeneous surfaces; however, it is being mentioned that the roughness must be at the molecular level and must be compared with the size of the droplet. The Cassie-Baxter and Wenzel models work when the roughness/heterogeneity is small compared with the liquid-vapor interface [16]. However, for research areas it is recommended to use inert probe liquids to conduct the measurements of the contact angles to avoid any interaction between the liquid and molecules at the

surface [17]. The theories are based in the fact that wettability can be modified by increasing the roughness and heterogeneities at the solid/liquid interface [18,19]. Wenzel's theory states that the surface roughness parameter is equivalent to the ratio of the actual area to the projected area of a rough surface. In Addition, roughness is small that has the ability of penetrating being in contact with the whole surface. The interactions between liquid and solid are strong completing a full wetting filling the grooves.

It is the opposite for the Cassie-Baxter effect since only a fraction of the droplet is in contact with the surface. The fraction of the water/solid area under the droplet is projected under the base of the drop. The Cassie-Baxter effect is useful for the analysis of heterogeneous surfaces that contain air pockets within the voids of the surface. Droplets partially sit in the air pockets, due to the random direction of the patterned surface where voids are filled by air as displayed in Figure 1. The new patterned surface and the air content increases the CA values. The air sheltering effect is based on the level of roughness, rougher surfaces entrap more air than flat surfaces eliminating the possibility of water droplet penetration/contact with the surface.

Suspension or collapse of the liquid droplet at the surface is based on the contact line density. This is based on the balancing of the surface body and forces produced by the weight of the droplet balancing body and surface forces at the contact line. The asperity or roughness of the surface must be meet to repel water molecules from the surface. Surface forces at the perimeter of the patterned edges (produced either by lithography methods, embossing or an actual collection of woven or nonwoven nano-micro fiber mats) must be greater and directed upwards. The asperities developed by the randomness of fibers must be at enough height preventing the sag made by liquid to reach to the bottom surface [19]. Exists several other models also based on nature mimicking the morphology of lotus leaf. The aim of the models is to develop the geometric pattern morphologies with micro-

nano pillars that will create a sort of roughness followed by the addition of hydrophobic coatings in form of fine branches creating a hierarchical effect on the surface.

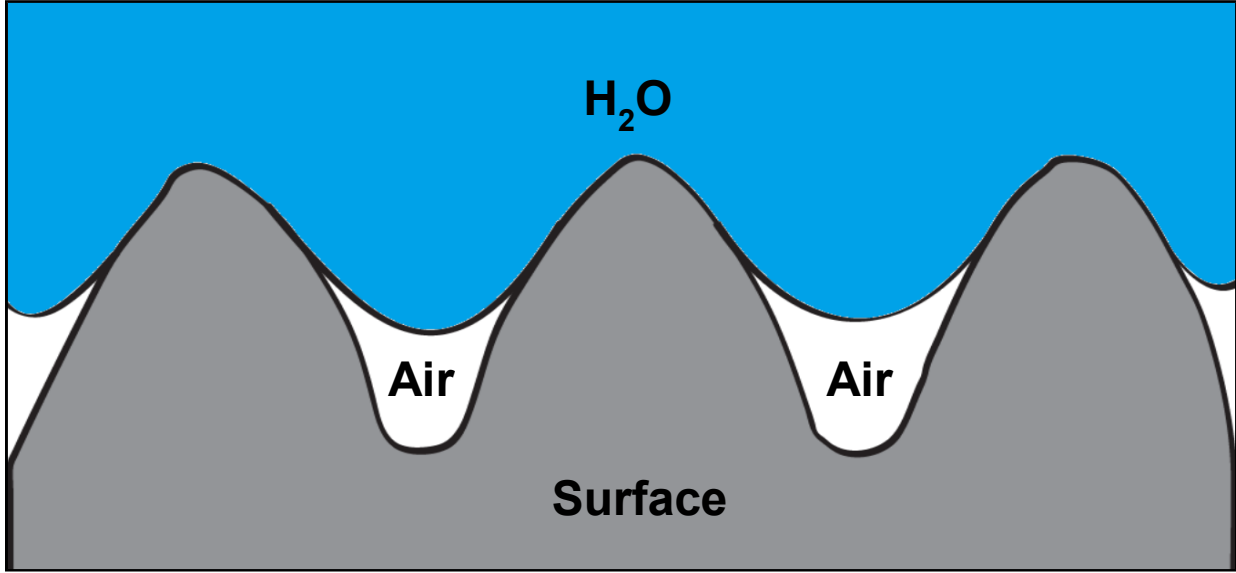


Figure 1. Cassie-Baxter Effect

Young's equation represents three different interfaces that are present during the equilibrium of the drop under the action of interfacial tensions:

$$\gamma_{lv} \cos \theta_Y = \gamma_{sv} - \gamma_{sl} \quad (1)$$

Where γ_{lv} , γ_{sv} , and γ_{sl} represent the liquid-vapor, solid-vapor and solid-liquid respectively and θ_Y is the contact angle. The dynamic CA is an important characteristic wettability in motion and obtained from the advancing contact angle θ_a and receding contact angles θ_r , respectively.

Contact angle values especially high contact angles that categorizes superhydrophobic surfaces are governed by morphological structures at the surface. Large number of studies have demonstrated that superhydrophobic surfaces are indispensable to address some of the current issues. The combination of roughened surfaces with extremely low surface energy is considered one of the simplest methods to manufacture superhydrophobic surfaces [20]. As mentioned above some plants and polymeric materials are hydrophobic in nature. The Lotus, *Nelumbo nucifera* leaf, in this case

has the most promising self-cleaning property due to the randomly micropapillae diameters from 5 μm to 9 μm . The great advantage of the micropapillae are their fine-branch nanostructures with diameters of almost 120 nm on the top and on the side of the pillars producing a hierarchical pattern. The existence of nano-micro structures at the surface results the formation of air pockets, resulting high CA values between the lotus leaf and water droplet. Waxes are being found on the surface of lotus leaf. The collaboration of surface nano-micro structures and hydrophobic waxes results a high-water CA and low tilting angle, exhibiting low-adhesion properties [21]. Since the introduction of Scanning Electron Microscope (SEM) studies had explained the morphology of lotus leaf and described the self-cleaning property. Some of the methods employed to generate superhydrophobic surfaces includes atom transfer radical polymerization (ATRP), chemical etching, chemical vapor deposition, electrospinning, hydrothermal approach, spin coating, chemical bath deposition, chemical bath deposition, and electrochemical deposition [13,21].

The values of contact angle define characteristics of the surface that describe important surface physical sciences that can be used to quantify and determine the ability of a surface to be in contact with an aqueous environment. Understanding surface physics within the interface can be defined by CA values. Work of adhesion, interfacial free energy and surface free energy are the most important surface characteristics for the development of self-cleaning surfaces. Work of Adhesion also known as adhesion strength considered a theoretical value that represents the amount of energy that must be applied to separate two phases adjoined to each other.

It represents the strength of contact between the two adjacent phases, in this case the droplet on the surface. It is important to obtain a general approach of the forces at the molecular level acting during the contact between two surfaces. High adhesion strength usually shows low contact angle values due to the strong interactions at the surface requiring larger amount of energy to detach the

surfaces. Value of work of adhesion provides an idea of the tilting angle since low values of work of adhesion is due to the low interactions at the surface. Exists many equations that can be used to calculate the work of adhesion based on theories correlated with the type of surface. Due to the heterogeneous surface developed by the random direction of fibers. Equation 2, is used in this study to determine the value of work of adhesion using the variables of surface tension of the probe liquids and contact angle measured.

$$W_a = (\gamma_l + \cos\theta) \quad (2)$$

Surface free energy is one of the most critical characteristics of understanding the wettability of nonwoven nanofiber mats. Surface free energy is considered as the excess of energy at the surface of liquid and solid. It is described as an attraction between molecules of the surface with molecules from the bulk due to cohesive forces. However, the molecules at the surface are pulled inward by the adjacent molecules with forces greater than attraction forces to the medium.

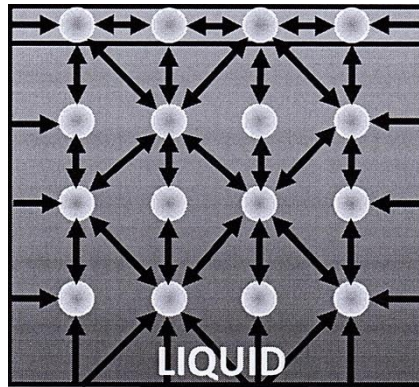


Figure 2. Unequal forces experienced by molecules at the surface of the liquid.

Due to such mechanism liquid shows a smooth surface behaving as a thin film, as it seems that the surface is under tension. Figure 2, demonstrates a graphical representation of intermolecular forces of molecules in the bulk and at the surface. In other words, surface tension in as effect within the outer layer of the surface behaving as an elastic sheet that allows insects to walk on the surface such as the water strider. When the liquid interfaces the solid produces the same effect resulting an

imbalance of molecular forces at the liquid, resulting a high attraction with molecules from the environment exerting a net force pulling them together as shown in Figure 3. However, high values of surface tension demonstrate a low interaction of molecules.

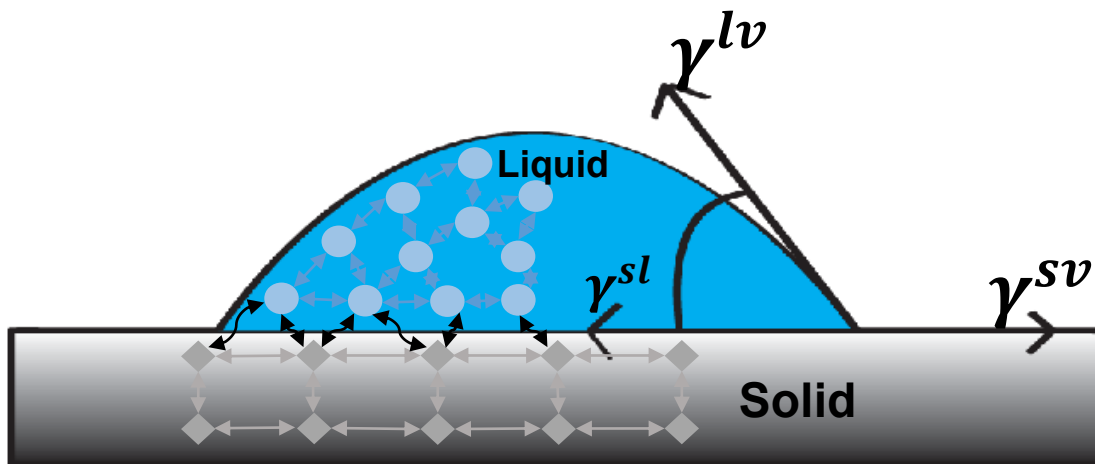


Figure 3. Intermolecular interaction of Liquid and Surface

Exists several theories of surface free energy that refers to the idea of dividing the energy into components based on the contact angle. The components are based on the intermolecular forces on the surface. Some of the intermolecular forces includes orientation force, inductive force, hydrogen bonding, and dispersion force. Orientation, inductive and dispersion are generally known as van der Waals forces. The theories of surface free energy have been developed with the purpose of expressing the components of work of adhesion using solid and liquid components. Having determined that components of surface free energy can be obtained based on the values of contact angle. In this study theory of acid-base is used to determine the amount of surface free energy using variables of LW and AB, Lifshits - van der Waals and Lewis acid-base component, respectively. The acid-base equation is given below:

$$\gamma_{lv}LW = \gamma^d + \gamma^i + \gamma^p \quad (3)$$

Equation 3 was used in this study to calculate the surface free energy of the surface based on its contact angle value based on the probe liquids used in the study. The component named as d is

defined as the dispersion force, component i as the orientation force and p as inductive force. Such components are derived from the idea of polarity or non-polarity. For example, dispersion force consists of the forces of interaction of non-polar molecules with dipoles generated by the electric dipole developed by vibration causing a distribution of electrons. In addition, orientation forces are developed when molecules orient with positive and negative charges. Molecules are neutral of electric charge, partially both positive and negative electric charges still exist due to the deflection of charges. Both charges can be attracted to either positive or negative charges orienting each other by a static electricity force. However, dipole forces are generated with a polar molecule when electric charge is closer to a non-polar molecule without a charge. The charge is inducted to the non-polar molecule developing a static electricity force; however, inductive forces are ignored in some theories due to the small size of their magnitude.

Interfacial free energy is just as similar as the surface free energy with the only difference that interfacial free energy within the interface. It explains the attractive forces between molecules of different liquids in the interface, usually expressed in units of J/m^2 . Droplets in contact with the surface finds its own equilibrium and conform based on the minimum total interface energy of phase boundaries. In the case of surfaces with high wettability, the interface of the liquid-vapor is less than the solid-vapor interfacial energy phase. It is important to find the general approach to the analysis or forces at the molecular level during the contact between two phases. For the development of ice phobic and antifouling surfaces work of adhesion is one of the most critical properties to describe the work or the amount of energy needed to remove a fluid from the surface. It has been demonstrated in recent studies that surfaces with low contact angle values, demonstrate low values of work of adhesion; while, surface with high surface free energy shows higher strength of adhesion [22].

2.6 Polymeric Nano-micro Fibers

Polymeric nanofibers have become an important area of study due to their potential applications in areas such as tissue engineering, filtration, barrier and protective fibers, sensors, pharmaceutical, contamination prevention, water repellency, self-cleaning, and biocompatibility [20,23]. Nanofibers attracted attention due to their remarkable properties, such as high surface area and high porosity [24]. Fibers collected at random directions entangles with each other creating small pores in between. The air content bridges out the surface from the contact of water, prohibiting spreading the water molecules on the surface. Fibers made of silk are considered a potential candidate for antifouling applications due to its powerful solubility performance in the marine environment [25]. Studies have demonstrated their potential application in coatings, it can be expected to dissolve at the water/surface interface resulting a self-cleaning surface.

Hydrophobic surfaces with high values of high surface energy tend repel water molecules and to accumulate microorganisms on their surfaces. However, hydrophilic surfaces encounter higher values of surface free energy increasing the opportunity of interacting with the environment, enhancing the attachment of organisms at the surface. As explained above, the fouling process can occur from a variety of conditions, such charge density, hydrophobicity or hydrophilicity. The wettability of polymeric systems can be altered by adding amphiphilic polymer chains which possess both wettability hydrophobic and hydrophilic sections. One way to address the antifouling ability is by decreasing the hydrophobicity of the surface.

The advantage of using natural fibers is their abundance at low cost, degradability, flexibility during the processing and machining, low density, high tensile and flexural modulus [26]. Natural fibers are usually added to polymers either thermoplastics or thermosets to create a fiber composite. The adhesion of natural fibers to the polymers is low, for this type of situations modifications either

by radiation, activation of functional groups or addition of coupling agents such as silanes, are used to promote interfacial adhesion to improve overall properties of the composites [26]. Compatibility of the fiber with the matrix is another factor to consider since the ability of the fiber to couple with the matrix of the polymer results the effectiveness of the bonding. The adsorption of moisture by the fibers can produce low interfacial adhesion between the fiber and the polymer causing dimensional changes of the polymer. One of the disadvantages of the fibers is low thermal stability due to their degradation that might take place and its wettability. The application of physical and chemical treatments to the reinforcing fibers may change the properties of the polymer, one of the most common cases is the transformation of the surface energy at the surface. Changing the wettability of the surface from hydrophobic to hydrophilic or vice versa that can be beneficial to adhesion bonding of the fibers with the matrix polymer. Chemical treatments relate to the change of the cell walls of the fibers modifying their stability, reducing water absorption, increasing its resistance to fungi growing in the fibers. Reducing its impact strength due to the embrittlement of the chemical agent during the treatment. Chemical treatments consist on the addition of coupling agents that tethers the fibers with the polymers creating a chemical bridge among the fiber and polymer matrix. The most common copolymers coupling agents are used for to create bridges between the fibers and polymer matrix are the maleated polypropylene (MAPP), and maleated polyethylene (MAPE). The advantage of using these two copolymers is due to their maleic anhydride groups that reacts with the hydroxyl groups of the surface creating ester bonds while the end of the coupling agent entangles with the polymer matrix due to their similarity of polar groups [26]. Silanes are also considered excellent coupling agents for natural fibers with polymer matrix. They are also being used as reinforce inorganic fillers with carbon and glass fibers. Silanes promotes a better adhesion between fibers and polymers producing a stronger adhesion with any adhesive setting that can be due to the hydroxyl

groups that also exists in carbon and glass fibers. Hydroxyl groups are some of common functional groups also encountered in fibers. The aim of using silanes as adhesion promoter is due to their ability to bond material with different similarities. It is silicon based polymer with four hydrogen atoms as part of its chemical formula. The advantage of the surrounded hydrogen atoms is that they can easily form covalent bonds with other atoms categorizing silane groups are widely used for many applications [27]. In the case where dissimilarities are too high or critical is necessary to perform primary treatments to enhance the bonding of the silanes on the surface ultimately producing a bonding between the two phases of fibers and polymer matrix. Silane groups have the advantage to adhere to type of surface, inorganic particle or substrate due to their ability of underacting with organic molecules and form covalent bonds with inorganic surfaces or substrates.

The application of membranes exists in many water filtration systems where their antifouling property is a priority. Pressure retarded osmosis process is highly utilized in membranes. In this technique, a solvent is separated from a concentrated solution, it has been used in industry for years, unfortunately still facing problems of antifouling on the membranes used for their filtration. Water treatment is another area where membranes are widely used. The problems are based on the accumulation of microorganisms, clogging of the membrane by the formation of an extra-cellular polymer substances (EPS) within the microbial cell matrix [28]. The deposition of the particles, colloids, macromolecules and salts is caused by the interaction of organic and inorganic compounds and biological substances. Fouling consists on the chemical degradation of the outer layer and could be controlled by the penetration or repulsion of all organisms in the environment. The outer layer of the material plays an important role due to its activity with the environment. To control the repulsion, permeation of organisms and substances in the environment could be an alternative way of

eliminating the fouling activity. Altering the wettability of the outer layer can be an alternative way of eliminating or reducing the activity of fouling.

The factors that can be considered and modified to control the fouling process of membranes are the electrostatic charge, roughness and hydrophilicity of the surface. Fouling process begins by the adhesion of microbial cells followed by the formation of EPS creating the conditioning film for the process of fouling [29]. Preventing the formation of the conditioning film is a priority to reduce the fouling on the membrane. The accumulation of organisms and substances from the environment developing the conditioning film provides higher surface free energies promoting attachment of organisms on the surface.

Membranes are usually fabricated with polymers that can perform well in the working environment especially the type of contact fluid, pressure and the type of organisms or particles in the fluid. To encounter all these properties, especial polymers are used for the fabrication of membranes. PVDF is widely use as the primary polymer for membranes in water treatments. One of the disadvantage of PVDF is its naturally hydrophobicity that results an essential property to minimize the fouling activity. Resulting a big water flux reduction and eliminating the material from water treatment activities. A way to modify the wettability of the surface is by the addition of hydrophilic monomers at the surface using several methods such as physical blending, coating, deposition, surface modification, chemical grafting, or blending with hydrophilic additives and interfacial polymerization [28,30]. Low surface free energy molecules travel to the surface leaving the bulk material covered. Such action of blending particles can be taken in consideration to control and modify the wettability of the surface. Several studies have reported blending of methyl methacrylate and PEO as additive. PEO is a hydrophilic polymer that can be used for many applications, D. Rana and coworkers added PEO to added to a poly (vinyledene fluoride) membrane

to increase the surface hydrophilicity of the membrane [31]. Other studies have added of hydrophilic macromolecules such as polyurethane to hydrophilic surfaces. However, the rendering of hydrophobic polymers results a hydrophobic surface. Similarly, the addition of both hydrophobic and hydrophilic polymers results a surface with enhanced antifouling properties. The addition of hydrophobic and hydrophilic polymers at the surface will produce fluorohydrocarbon molecules that will result in a sort of lubricant that eliminates the fouling activity of microorganisms and proteins at the surface.

Other studies have altered the surface by adding nanoparticles to enhance pore connectivity of the primary polymer with the hydrophilic material. Ultimately, increasing the water flux and permeability of the membrane by the hydrolyze reaction of nanoparticles with the environment. One of the approaches for an effective antifouling membrane can be accomplished by the arrangement of molecules of the polymer at the surface. It is being demonstrated that organisms are trapped in the gaps formed by the arrangement of molecules at the surface [32]. On several applications fouling mechanisms is due to the hydrophobicity of the surface. Hydrophobic surfaces tend to accumulate microorganisms due to their higher surface tension values.

As mentioned before, non-woven nanofiber mats have the potential to be used as antifouling. The ability of manipulating the architectures with fiber diameter, porosity, and or intrinsic arrangement of leads to lower the interfacial bond between biofoulants and surface and promotes easy removal by a low shear forces produced by the hydrodynamic shearing force as the ship displaces [33]. The advantage of using non-woven mats is their high surface area to volume ratio at the nano-scale level. Jeffrey G. Lundin and coworkers performed a study using this property of nanofibers. Their study consisted of adding biocides such as Quaternary ammonium salts (QAS) in the preparation of polymer solutions of Nylon and Polycarbonate (PC). It was quite significant

noticed that addition of QAS demonstrate effects in the fabrication of nanofibers for non-woven mats. All properties of fibers, including physical properties such as morphology, diameter are dependent in the parameters of polymer solutions such as viscosity and molecular weight. The major differences on the fibers, especially for PC was the diameter of the fibers. Considering that the diameter of the fibers is dependent in several factors of the polymer solution, in the electrospinning technique fiber's diameter is dependent in the conductivity and the viscosity. On the work of Jeffrey G. Lundin the addition of QAS increased the conductivity of the solution resulting an increased in the charge density of the polymer. High density charge solutions in the electrospinning technique increases the electrostatic repulsion forces facilitating jet movements and therefore stretching to form fibers [34]. On their study, it was noticed that PC nanofiber with QAS showed smoother surfaces than the control PC nanofibers. Such change in morphology may be due to the continuous evaporation of solvent during the fiber fabrication process. Changes on the diameter and morphology of nanofibers is a result of the solution conductivity. In the case of Nylon, it was the opposite, nanofiber diameter increased from 91 nm to 193 nm in the case for one of the QAS additives. The increment of diameter was due to the increase of viscosity, even though the conductivity of the solution increased by the addition of QAS the diameter of the fibers increased due to the reduction of the charge density. Since the repulsive forces were minimum less movements and stretching actions were experienced by the fibers ultimately the diameter of the fibers remain relative large [34]. Both kinds of nanofibers were subjected to bacteria environments, *S. aureus* bacteria to study their activities. Nylon with QAS showed the highest rejection of bacteria even though the diameter of the fibers increased by the addition of QAS. The addition of nanoparticles to the non-woven mats is one of their greatest advantages and can be used in several applications. Aravind Dasari and coworkers performed a study where nanoparticles containing biocide were introduced to the

membranes. The aim of their study was to develop antifouling membranes preparing non-woven mats made of nanofibers with electrospinning technology. Polylactic acid (PLA) was used as the precursor. PLA is a hydrophilic polymer with potential to produce an antifouling response given the formation of a hydrated layer on its surface. Silver (Ag) and Copper (Cu) were used given their biofoulant activity. These were functionalized with sepiolitem (Sep). Sep is a metallic nanoparticle support. In this study a silicate matrix content was functionalized with Ag and Cu nanoparticles and added to the solution of PLA for fabrication of nanofibers. SEM images demonstrates that Ag and Cu nanoparticles were embedded into the matrix of silicate due to the collapse action of Sep structure over the nanoparticles during the functionalizing process. The aim of their study was to develop antifouling membranes by adding the biocides in the polymer solution. One part of their study was to keep the membranes in a cross-flow configuration media with bacteria suspended. *Saccharomyces Cerevisiae* and *Pseudomonas putida* were the predominant bacteria on the study. Membranes showed a >98% rejection on particles exceeding 3 μm determined by the particle counting. ATP assays were performed on the study to determine the active biomass at the surface. According to the ATP results Ag and Cu functionalized Sep showed lower adhesion of biomass with respect to PLA. Ag-Sep membranes demonstrated the lowest adhesion of *S. cerevisiae* bacteria on the surface 85 % reduction of adhesion. Cu-Sep showed lower bacteria adhesion as well, but still Ag-Sep performed better with *cerevisiae* bacteria. The addition of Ag and Cu fibers increased the permeability of the membranes approximately twice as much as regular PLA [35]. A similar work was performed by Hengchong Shi and coworkers. Their study consisted of adding silver (Ag) nanoparticles into Polyurethan-g-polyethylene (TPU-g-PEG) due to their high activity against bacteria and parasites. Ag nanoparticles encounters the possibility of destroying the metabolic process of the growing and proliferation of bacteria on any surface. Surfaces coated with Ag nanoparticles demonstrated the ability of killing

several pathogens such as gram positive human pathogens (*Staphylococcus aureus*) and gram negative bacteria (*Escherichia coli*). Their work was a little different than the previous, TPU electrospun fibers were dipped coated with PEG followed by a second dipping coating with Ag nanoparticles. Ultimately developing a TPU-g-PEG/Ag electrospun nanofiber membrane. According to their contact angle values, it seems that the addition of PEG developed a hydrophilic surface on TPU, the contact angle went from 25.9° to 9.9° due to the hydrated layer formed by the water molecules of PEG. Bacterial studies with gram-positive bacteria *S.aureus* and gram-negative bacteria *E. coli* were conducted. The samples were exposed to the bacterial environment for 24 hours. It was shown that bacteria showed a tendency to attach to hydrophobic surfaces, the hydrophobic surfaces of TPU and was highly proliferated by *S. aureus* bacteria. However, the TPU-g-PEG and TPU-g-PEG/Ag surfaces demonstrated ~98.9 % and ~95.1 % reduction of *S. aureus* bacteria compared to the hydrophobic TPU. Such effect could be by the addition of the antifouling hydrated PEG on the surface resulting in a hydrated layer reducing the overall surface free energy of nanofibers [36].

The ideal process would consist on the segregation of polymer assemblies combining antifouling agents and low surface polymer chains. One of the most common polymers added or tethered onto polymer chains is poly (ethylene glycol) (PEG), a hydrophilic polymer that promotes a hydration layer that inhibits the attachment of microorganisms to the surface due to its low value of surface tension.

One of the most common hydrophobic polymers used for antifouling applications especially used for the fouling release mechanism is PDMS. In the transformation of liquid polymers into fiber form several parameters must be taken in consideration such as concentration, molecular weight, and viscosity PDMS and PEG fiber blends were studied by Tungprapa and coworkers. The addition

of PEG increased the viscosity resulting nanofibers large fiber diameter [35], which also influenced on the collector distance.

In the marine environment exists thousands of organisms and plants that can be attached to the surface; however, algae, bacteria and barnacles are common marine plant and organisms that seek metal surfaces to grow and proliferate. PDMS and PEG systems could promote the development of antifouling surfaces due to their fouling release mechanism, resistance to protein adsorption and cell adhesion.

A common method of reducing the fouling activity on the surface is by increasing the roughness of the surface. Rough surfaces provide lower surface energy therefore decreasing the possibility of microorganisms to attach to the surface. In addition, the roughness of the surface increases the fluid flux through the membrane. However, in the case of colloidal particles that seeks out for valleys and groove on rough surfaces, this can then be counter-productive. Colloidal particles would nicely deposited [37]. Deposition of organic particles on the surface in the first fouling process, organic particles provides higher surface free energy and consequently attract more organisms to the surface. Smoother surfaces do not provide such types of shelter to colloidal particles due to their lower surface available, therefore eliminating the chances of sheltering of particles on the surface. Surface treatments that consists on the addition of particles to the surface are considered a method of increasing the roughness of the surface. New particles attach to the surface forming a new layer of material with tailored functionality.

CHAPTER III

EXPERIMENTAL PROCEDURE

The aim of the study is to determine the physical and chemical properties at the interface of two or more phases. In the case of nonwoven systems, physical and chemical properties at the interface are highly dependent on the morphology and diameter of the fibers. Fibers were produced using the Forcespinning® technology. Nonwoven fine fibers mats were developed from several polymeric systems such as Nylon6, polyvinyl difluoride (PVDF), polytetrafluoroethylene (PTFE), polypropylene (PP), thermoplastic polyurethane (TPU), polybutylene terephthalate (PBT).

Nylon6 can be used in many applications due to its advanced mechanical properties compared to other polymeric and synthetic materials. Nylon6 exhibits both crystalline and amorphous phases, amorphous consisting of isotropic and anisotropic areas [38]. The crystalline component has two crystalline forms, α -form and γ -form and its formation is highly dependent upon processing conditions. The crystal α -form consists of enlarged chains with intra-sheet hydrogen bonding; while, γ -form consists of pleated chains with inter-sheet hydrogen bonding. Hydrogen bonding from the polymeric molecules determines the wettability of the surface based on the interactions with hydrogen from the water molecules. An advantage of Nylon6 is its stability with body fluids that can be a potential candidate for bone tissue engineering. In Addition, Nylon6 has been adopted by the biomedical and textile industries as a medical polymer for artificial skin and clothing, respectively [23]. Similarly, Nylon6 is been considered as an alternate polymer with high

spinnability that simulates bone collagen chemically and structurally due to its backbone structure stability in human body fluids [39,40].

PVDF has been intensively explored by different industries for several applications due to bulk properties of high electric resistance, light weight and hydrophobicity. Properties that had been increasing the applications of PVDF for several applications such as air cleaning ultrafiltration, microfiltration [24]. Extensively research regarding the possibility of implementing PVDF nanofibers for rechargeable batteries, due to its ionic conductivity improving cell rate capability [41].

3.1 Forcespinning Technology

Forcespinning® (FS) technology was developed at the current university (UTRGV) previously known as UTPA. FS is one of the latest technologies for the fabrication of fibers besides electrospinning, melt blowing, centrifugal spinning, liquid shearing and most recently magneto spinning [42]. The advantage of FS technology relies on the fiber yield and broader selection of materials that can be converted into fiber coupled with an environmental friendly process. Conductive and non-conductive solutions can be used given that the process relies on the use of centrifugal forces rather than traditionally used electric fields. The forces act in the perpendicular direction of the rotational speed resulting the ejection of the polymer solution from the spinneret. Nanofibers are advantageous for a large number of applications due to their high surface area, high length/diameter ratio, surface morphology, flexible surface functionality and superior mechanical performance [36].

3.2 Contact Angle

The CA is defined as the intersection of the liquid-vapor-solid interface, geometrically acquired by applying a tangent line from the point of contact along the interface of the droplet profile.

Small quantities, sessile drops of liquid are manipulated on the surfaces. Correctly, the shape of the droplet is determined by the surface tension of the liquid. In the bulk area of a liquid, each molecule is pulled equally in every direction by its neighboring liquid molecules resulting a net force of zero. Meaning, the molecules are pulled inwards by its own neighbor molecules producing an internal pressure maintaining their lowest surface free energy in the bulk. Such intermolecular forces contract the surface, which is called surface tension. Surface tension is mainly the force driving the shape of the liquid droplets. In addition, external forces such as gravity deform the droplet; consequently, the CA value is resolved as the combination of surface free energy and external forces such as gravity.

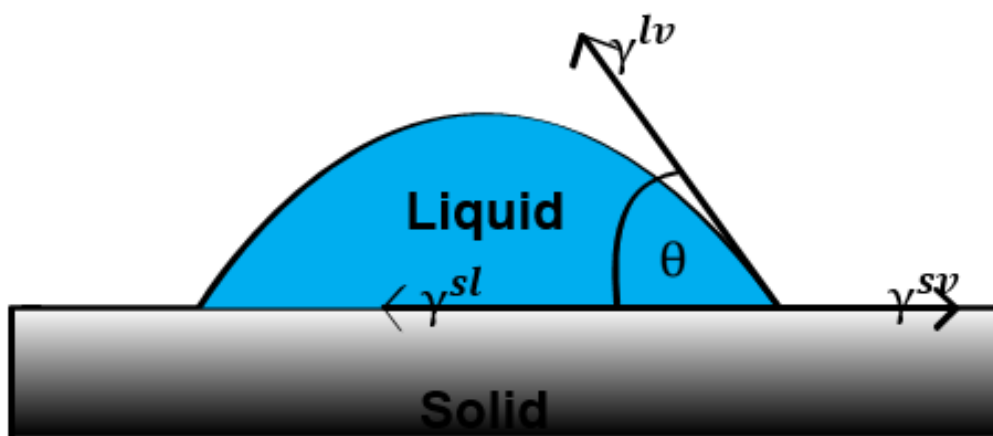


Figure 4. Contact Angle

Theoretically, the CA can be considered a value that represents characteristics for a given liquid-vapor-solid system in a specific environment. Figure 4 demonstrates the CA between a liquid drop and a solid surface.

Advancing and receding contact angles are considered as the maximum and minimum contact angles that the liquid on the surface can approach [19]. Dynamic contact angles can be measured at different speeds for a specific environment. The difference between the advancing and receding contact angles is called the angle hysteresis. The significance of the contact angle hysteresis is critical to consider on the designing of surfaces with low wettability. Hysteresis is related to the

surface roughness and nonhomogeneous surfaces. In the case of nonhomogeneous surfaces, a specific feature forms a barrier to the motion of the contact line. In the case of hydrophobic and superhydrophobic surfaces features will form a sort of pinning prohibiting the motion of the water droplet when it recedes, increasing the value of the contact angle. Contact angle hysteresis is usually seen in nonhomogeneous surfaces; experimental contact angles are only seen on homogeneous surfaces. In Addition, experimental contact angles are based on the Young's equation, eq. (1).

3.3 Scanning Electron Microscope

The Scanning Electron Microscope (SEM) from Sigma VP Carl Zeiss was utilized to carry out the study of the morphology of the fibers and nonwoven mats SEM is one of the greatest technologies used to characterize surfaces in the micro-nano scale, displayed in Figure 5.

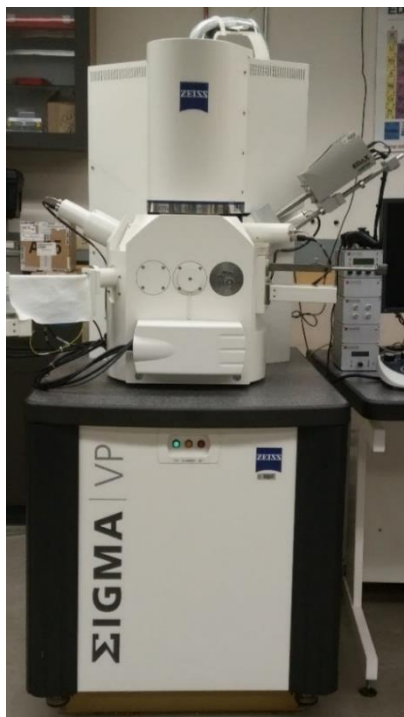


Figure 5. Scanning Electron Microscope

It consists of several components such as lenses, electron beam, analysis chamber, secondary electrons (SE) and backscattered electrons (BSE). The electron beam is one of the most critical

components of the SEM, since it generates the electrons that are focused into a narrow beam that scan across the sample. The generation of electrons consists of having a current running through the anode becoming extremely hot that the electrons boils out from the metal. Once the electrons are generated within the filament, a voltage is applied creating an electric field that pulls out the electrons from the tip of the filament, such process is called field emission. The electrons coming out from the filament goes through the lenses to be guided and collected before being sprayed down. Within the lenses exists an electron-magnet that is winded in a coil embedded inside the iron ring. Since the electrons go through different components within the electron gun, the purpose of the electron-magnet is to collect almost all electrons and bend them towards a single point below the lens. The purpose of the electron-magnet is to group the electrons together; it usually creates high magnetic field due to the current being applied. The magnetic field enlarge resulting an effect of bending the electrons inward tightly together. Once the electrons enter the magnetic field a perpendicular force is applied at the electron that pushes them towards the axis of the lens. Such inward force changes the direction of electron beam the same way the lens focuses the light. The beam of electrons passes through an aperture on a plate to skim out the electrons that were not tightly focused. The electrons pass through another set of lens and orifice to further narrow the electron beam resulting a parallel electron beam shape. In the final focusing, the lens encounters two additional electron-magnets where current is pulsed through the coils producing an oscillating magnetic field that collects and guides the electron beam across the sample surface. The electrons coming out from the sample hit the surface, electrons with high-energy bounce back out of the surface, such electrons are called backscattered electrons (BS). The electrons knocked out of the sample are called, secondary electrons (SE); electrons from the sample are counted by detectors. Electrons are sorted according to their high energy, SE electrons are usually lower in energy;

however, BS electrons are high in energy. The detector collects just the electrons that reaches in the energy level.

Inside the detectors, electrons first strike a scintillator plate where photons are kicked out. The photons are created by the phosphor atoms that are incorporated into the scintillator plate, the atoms convert the kinetic energy of the electrons to light energy. The photons created move along a channel until reaching to an electron multiplier. Inside the electron multiplier, photons remove out electrons that moves into a curved metal plates. A single photon produces millions of electrons due to the gradual increase of energy throughout the plates. Electrons kicked out at the first plate, at low energy, accelerates into the further plates where each one kicks out multiple electrons. This multiplication of electrons continues downward the same way the avalanche grows. All signal from the detectors are sent to the CRT, where the brightness of the image spot is controlled. A circuit generates a signal to scan both the SEM electron beam and the CRT spot. When the signal is on the way to the SEM it passes through gain amplifiers.

The CRT spot follows a synchronized path, every time the electron beam passes through feature on the surface that releases a big number of electrons, such electrons are collected and amplified by the detector producing a brighter image on the screen by the CRT spot. Due to the synchronized path followed by the CRT spot an image of the scanned feature is represented on the screen.

SEM functions under vacuum pressure by running a venting process injecting nitrogen gas to removing out all type of molecules and gases from the analysis chamber. The technology consists of an electron beam that is position on the desired area of analysis. The electrons generated by the electron beam starts to hit the atoms on the surface. The electrons of the outer shell from the atoms on the surface leave the atom after going through an excitement process based on the energy received

by the electrons generated from the beam. Due to the interactions of the electrons with the atoms from the surface, it reveals high resolution images from the surface. Figure 6, demonstrates a simplified diagram of SEM and all the components.

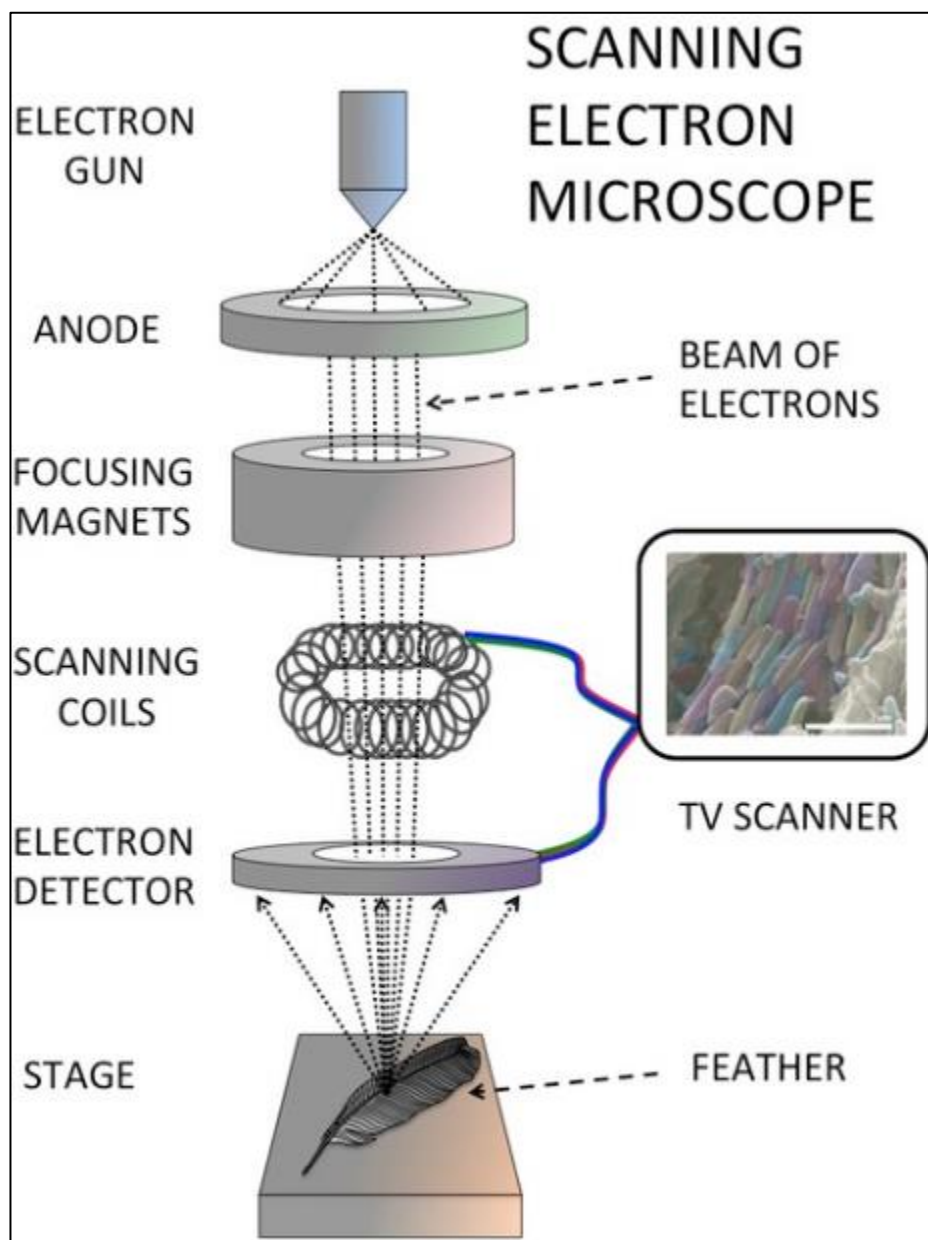


Figure 6. Simplified Diagram of SEM (prehistoric-colours-blog)

3.4 Manufacturing Parameters

The aim of FS technology is to produce fibers using centrifugal forces produced by the rotational speed of the spinneret containing the solution. As the spinneret rotates ejecting the solution

through orifices of the needles. The solvent evaporates converting the polymer into a fiber. The key parameters that controls the geometry and morphology of nanofibers includes, rotational speed, distance from collection system to spinneret and polymeric solution concentration. The control and optimization of these parameters allows the manipulation over the development of fibers with varying diameter, pore size, morphology and chemistry.

3.4.1 Polymeric Solution Concentration

Polymer solution concentration determines the ability of transforming the polymer into fiber form. The concentration of solution strongly influences the viscosity of the solution, low concentration results lower viscosity with low fiber production rate, and the presence of beads. However, solutions with high viscosity produces thicker fibers at higher speeds, beads might be present due to the limited fiber elongation. Solution shall not be overly concentrated or diluted; but, at least having enough concentration to form the fiber jet. Over concentrated solutions unable the possibility of fiber formation the flow rate of the solution will be out of the margins of control. Resulting, the inability of the formation of fibers of any diameter [43]. The miscibility property of the polymer/solvent is crucial to determine the morphology of fibers. One of the common issues is the volatility of some additives that reduces solvent evaporation, reducing the solvent evaporation leading to wet fiber formation. High volatile solvents increases the rate of evaporation in their corresponding gaseous or liquid phase, leaving only a solid phase which will in turn increase the surface area [42]. Faster evaporation of solvents produces a wrinkle pattern on the surface of fibers, increasing the surface area and air content at the surface.

3.4.2 Rotational Speed

Fiber morphology, porosity and diameter are managed by the rotational speed of the spinneret. Diameter of fibers is directly proportional to rotational speed with high viscous solutions.

The presence of beads might occur due to the inability of fibers to dry completely by the time it reaches the collector. Resulting the entanglement of fibers forming different shapes [43]. Fibers ejected at their optimum flow rate will have cylindrical cross-section.

3.4.3 Distance from Collector System to Spinneret

The distance between the collector system and spinneret influences the morphology and diameter of the fibers. Longer distances between spinneret and collection system produces higher elongation, therefore smaller diameters. The presence of beads may increase as the distance is reduced due to the inability of the fiber to dry before reaching the collector. The distance of collector determines the diameter of the fibers. Fiber collector close to the spinneret leads to smaller diameters due to the lack of elongation of the polymer jet resulting the formation of beads due to the lack of drying time. In Addition, FS technology is recognized for its high fiber management system that allows fiber collection ensuring a precise cross directional uniformity of fibers [44]. FS technology offers a great selection of polymers that could be used for the formation of fibers; however, process parameters are extremely important for their fabrication and efficiency.

3.5 Contact Angle Meter

Wettability plays an important role in industrial processes such as oil recovery, lubrication, coatings, fouling and printing. In the recent years, the interest in the study of superhydrophobic surfaces has been increasing. Due to their potential applications, such as self-cleaning, nanofluidics, icephobic and antifouling. Wettability studies normally involve the measurement of the CA as their primary set of data. Indicating the degree of wetting when a solid and liquid interact once in contact. Small contact angles $\ll 90^\circ$ corresponds to hydrophilic materials due to their high wettability. However, large contact angles $\gg 90^\circ$ corresponds to hydrophobic surfaces due to their low wettability. For superhydrophobic surfaces, usually their CA are greater than 150° demonstrating

almost not contact with the surface. The value of CA determines the wettability and categorizes the surface per their degree. The relationship among the surface and interfacial energies quantifies the behavior of a liquid and a solid surface considering the phase morphology of two or more phases present.

In the development of surface engineering it is important to take in consideration surface free energy, work of adhesion and interfacial free energy. All these properties must be quantified based on the values of contact angle to study the properties of the surface.

CHAPTER IV

EXPERIMENTAL SET UP

4.1 Polymeric Solution Preparation

For the most part, the materials used for study were Nylon6 ($\text{C}_6\text{H}_{11}\text{NO}$)_n and polyvinyl difluoride (PVDF) the solvents were of Formic acid (FA $\geq 95\%$) and N,N-Dimethylacetamide (DMC $\geq 95\%$) purchased from Sigma-Aldrich (St. Louis, MO, USA) while Acetone ($\text{C}_3\text{H}_6\text{O}$ F.W. 58.08) was purchased from Fisher Scientific. Other fiber systems such as polyvinyl difluoride (PVDF 5 and 8 GSM), polytetrafluoroethylene (PTFE), polypropylene (PP), thermoplastic polyurethane (TPU), polybutylene terephthalate (PBT) were obtained as is from Fiberio Technology Corporation.

Nylon6 solutions with concentrations of 23 wt.%, 25 wt.%, and 27 wt.% were prepared by dissolving the polymer at room temperature (RT) with FA solvent. The solutions were settled for 24 hours without mechanical stirring. PVDF solutions with concentrations of 20 wt.%, 22 wt.%, and 24 wt.% were prepared by dissolving the polymer in a 1:1 by volume mixture of N, N-Dimethylacetamide and Acetone. The solutions were mechanically stirred for 2 hours in a silicone oil bath. Followed for 2 hours of mechanically stirring at room temperature.

4.2 Fiber Fabrication

The fibrous mats of Nylon6 and PVDF precursors from different solution mixtures produced by FS technology. As aforementioned, FS technology ejects the polymer solution from

the spinneret. 1.5-2.5 milliliters of polymer solution were injected into the needle-based spinneret supplied with 30-gauge ½-in. needles. Rotational speed varied for the two different precursors. The rotational speed for Nylon6 solutions was 8000 and 10000 rpm for a spinning time of 5 minutes. However, the rotational speed for PVDF solutions was 7000 rpm spinning time of 5 minutes as well. Fibers were collected using a hand collector square-shaped from the collection system every two runs approximately; needles were changed after each run. The fibrous mats were removed from the hand collector and were covered and stored prior to being characterized.

4.3 Fiber Collection

The target collectors were located 6.5-in. from the tip of the spinneret. All collectors were screwed in the circular base as displayed on Figure 7. The base was placed in a circular port located in a lower area under the height of the spinneret. Providing enough clearance for the spinneret to freely rotate inside the inner the diameter of the base. There was a separation of 3.5-in. between collectors, same distance from the spinneret through all resulting a uniform formation of fiber web. Fiber mats were collected through the spaces in between each individual collector, producing 8 different collections every two runs approximately.

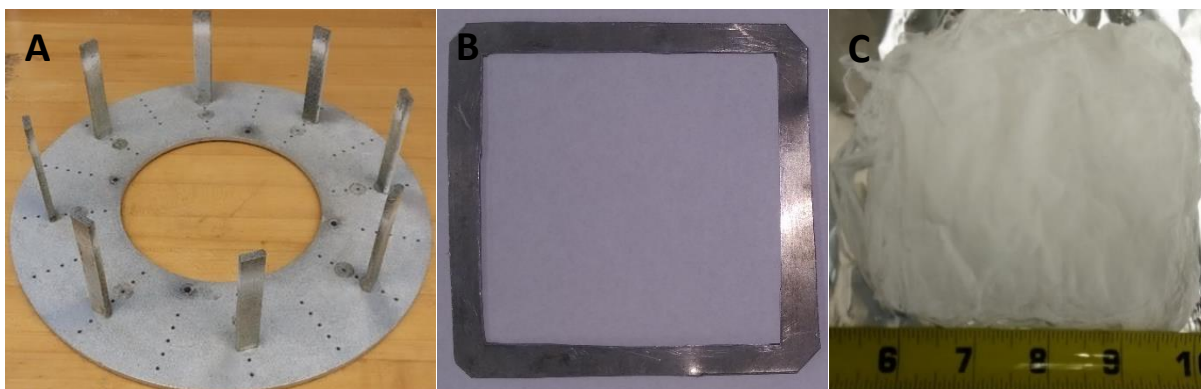


Figure 7. A) Fiber collection system, B) Collector and C) Fiber mat

4.4 Scanning Electron Microscope

Structures of fibers materials were examined using the Scanning Electron Microscope (SEM). Samples were sputtered with a thin layer of gold to enhanced the conductivity of the fibers. The metallic layer enhances the interaction of the electrons from the outer shell with the electrons generated by the electron beam. The electrons from the outer shell leaves the material and once quantified represents. Figure 8, shows the samples inside the sputtering machine after the deposition of gold on the surface.



Figure 8. Sputtering Fibrous Materials

4.5 Contact Angle Measurements

The purpose of measuring the contact angle between a surface and a water droplet is to determine the wettability of a surface. Measuring the angle in between the tangential line of the droplet in contact with the nonwoven mat. In this study the measurements of the contact angle performed on sample from nonwoven nanofiber mats with a uniform thickness. Figure 9 (A), (B) demonstrates a nanofiber samples cut from mat and contact angle meter used to determine the contact angle value, respectively. An automatic contact angle, DropMaster from KYOWA was used to report the static water contact angle using the sessile drop method. Recordings made by

measuring 3-4 μL water droplet size depositing it on the surface. Once the droplet is in contact with the surface it takes a time to stabilize due to the interactions made by the molecules from surface with molecules from the liquid.

The value of contact angle is determined by selecting the points on the images taken using FAMAS add-in software as shown in Figure 10. The camera from the instrument take images of the curvature of the droplet sitting on the surface. The purpose of the images is to select the tangential lines of the curvatures to the horizontal line. If it the curvature is a complete spherical form, the measuring lines can be positioned around the sphere to determine its value; Figure 10 also demonstrates the selected areas in an image to measure the contact angle. The determined by considering 10 different averages, each one made by 10 values of contact angle taken randomly on the surface at room temperature.



Figure 9. A) Contact angle meter and B) Fiber mat

Measuring the contact angles of nonwoven nanofiber mats is significantly different from smooth surfaces due to the heterogeneities produce by random direction of fibers at the surface.

Low-bond axisymmetric drop shape analysis for surface tension and contact angle measurements of sessile drops (LBADSA) was used. The analysis consists of solving the Young-Laplace equation per photographic images of sessile drops. The calculated drop curvature is enlarged by mirror symmetry so the reflection of the drop allows the position of contact points. A cubic B-spline interpolation is applied to the image reaching to the resolution of pixels [45].

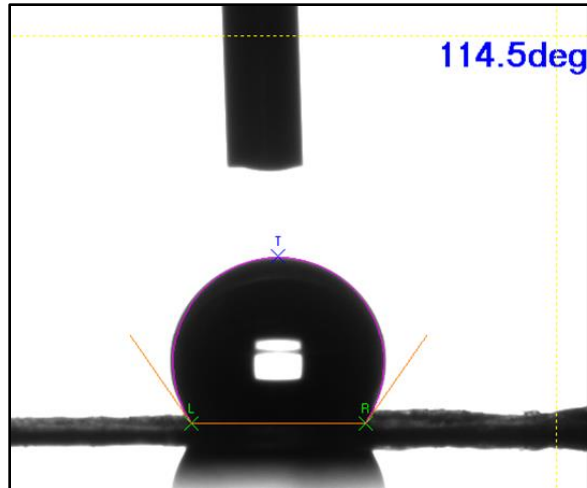


Figure 10. Points of selection for Contact Angle

Figure 11, demonstrates a graphic representation of the mirror symmetry of droplet at the surface. The software consists of taking a second order polynomial of the curvature of droplet. The result is a closest estimate of the actual contact angle between the horizontal surfaces with the tangential line of the droplet.

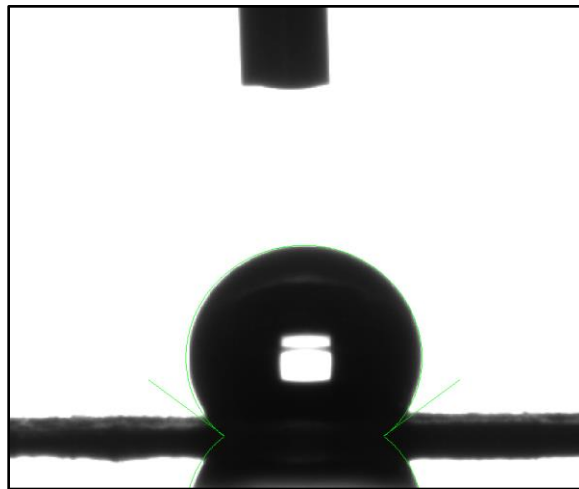


Figure 11. LBADSA

Contact angle values is the first step to determine the physical sciences at the interface of two of more phases. Obtaining the most exact values of contact angle leads to the most effective values of physic sciences such as surface free energy, work of adhesion and interfacial free energy.

A corresponding series of probe liquids with a predefined value of surface tension and density were used for the analysis. Probe liquids encounter the ability of having a minimum activity between molecules of surface and liquid. Using predefined values of surface tension is an easy method to determine the values of surface physics such as surface free energy, interfacial free energy and work of adhesion. Water is the most used probe liquid; exists dozens of liquids are being used. Liquids with different surface tension values can determine the critical surface free energy of solids. In addition, probe liquids of different molecular volume can identify the dimensions of nanopores in monolayers [46].

Figure 12, demonstrates the different probe liquids used in the analysis. Three different liquids were used for the analysis, resulting in a Ternary (3 component analysis) creating a combination of solid samples with three kinds of probe liquids. FAMAS built-in software considers the values of surface tension and density of probe liquids and determines physics parameters values based on surface tension and contact angle values measured and recorded. Table 1, contains the density and surface tension values of the probe liquids used for the analysis. The values of surface tension at 20°C except for Diiodomethane at 25°C. Surface tension values demonstrate the bonding cohesive forces among liquid molecules. In the bulk area of a liquid, each molecule is pulled equally in all directions by adjacent molecules, resulting in a zero-net force due to the balancing of forces within the molecule. Giving more freedom to molecules at the surface to interact with the environment. Table 1, also demonstrates the density values of each probe liquid. Density is a critical value to consider since due to the gravity force, it becomes a weight, consistently applying a force on the contact areas of the solid.



Figure 12. Probe Liquids

Table 1. Density and Surface Tension of Probe Liquids at certain Temperature

Probe Liquid	Temperature (°)	Density (g/mL)	Surface Tension @ 20°C (mN/m)
<i>Hexadecane</i>	20	0.777	27.47
<i>Ethylene Glycol</i>	20	1.120	47.7
<i>Formamide</i>	20	1.138	58.2
<i>Diiodomethane</i>	25	3.325	50.8
<i>Distilled Water</i>	20	0.9982	72.8

4.6 Evaluation of Algae Attachment

The evaluation of algae study is an ongoing study where the interaction of algae on the surface of nonwoven nanofiber mats is being evaluated. PTFE, and PP nanofiber mats were chosen for this study to compare and understand their interaction with algae. The algae was collected from a boat belonging to the University of Texas Rio Grande Valley as demonstrated in Figure 13. The collected algae were divided in two different mediums to identify the one that provides the most efficient environment for algae growth and proliferation, as shown in Figure 14. The flasks were placed on a warm illuminated environment providing the most naturally environment growth. After obtaining a homogenous number of algae cultured, nonwoven nanofiber mats PTFE and PP were placed in petri-dishes to introduce algae to culture onto their surfaces. Figure 15, shows the (1.5 x 1.5) cm mats in contact with algae.

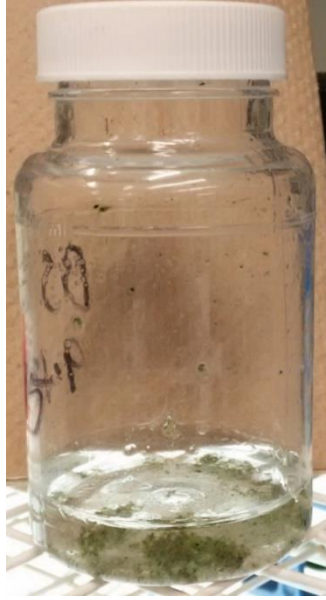


Figure 13. Naturally collected Algae



Figure 14. Culture of Algae in different mediums

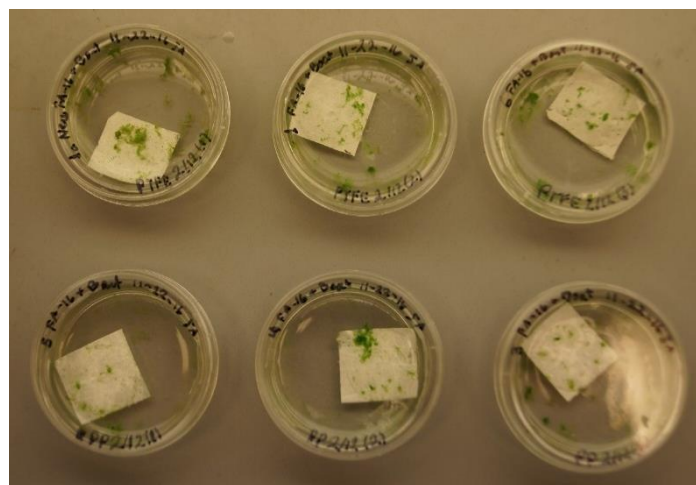


Figure 15. Algae study with PTFE and PP

The study will consist of a 7-day time point. The nanofiber mat will be soaking in a solvent N, N-Dimethylformamide (DMF) to extract all the algae attached on the surface of the mat. Followed by analyzing the medium using the spectrophotometer to determine the amount of chlorophyll in the solvent. Algae is considered a plant marine containing chlorophyll, cell plant that absorbs light to form energy. The spectrophotometer measurements consists of applying a spectrum of light to medium to analyze. Chlorophyl will absorb that light and by changing their color the results will be recorded by the instrument.

CHAPTER V

RESULTS AND DISCUSSION

The wettability of fine fibers (small fiber diameter, small pore size) is strongly dependent on the Cassie-Baxter mechanism. In the case of these materials, the pore size is also strongly dependent upon the aerial density, measured as Grams per square meter (GSM). The higher the GSM smaller the pore size. The Forcespinning® technology produces fiber with small diameters and study the GSM of the collected mats can be tailored to suit desired applications. This study focuses on the effect on the wettability according the fiber diameter and GSM. Several techniques were employed to characterize the morphology of the nonwoven nanofiber mats and their wettability [42].

5.1 Morphology of Nonwoven Polymeric Nanofiber Mats

Figure 17 demonstrates the SEM images of all fiber mats used in the study. The images depict clean homogeneous fibers, for example no beads are present. Nylon6 SEM images are shown. According to the morphology shown by the images, and based on the forcespun parameters, fibers provided an excellent morphology under the polymeric concentrations and collector distance. However, it has been determined from a previous study that solution viscosity by polymeric concentration of 15wt.% is too low to form polymeric nanofibers [47]. Fortunately, all chemically polymeric concentrations were above the previously mentioned value. Nonwoven nanofiber mats fabricated with Nylon6 of (20, 38, 41, 47, 49, 55, 72) GSM as shown at Table 2

demonstrates a systematic increasing of fiber diameter at (0.14, 0.75, 0.47, 0.63, 0.64, 0.54, 0.66) μm , except for 38 GSM and 55 GSM showing unsystematic fiber diameter values. Similarly, the morphology of PVDF 5 GSM, and 8 GSM, respectively. Based on the morphology shown by the image the polymeric concentration including manufacturing parameters were closed to the optimum characteristics showed by the absence of beads and defects on fibers. SEM images are also shown for PVDF 20wt.% (111 GSM), 22wt.% (75 GSM) and 24wt.% (114 GSM) forcespun at 7000 rpm. The velocity parameter of manufacturing was constant for all three nanofiber mats. Due to the small variation of solution concentrations the viscosity of each solution significantly influences the fiber diameter for all three surface mats. Table 3 demonstrates fiber diameter of PVDF 20wt.% (111 GSM), 22wt.% (75 GSM) and 24wt.% (114 GSM) with values of 1.73 μm , 1.74 μm and 1.81 μm , respectively. Exists a strong correlation between fiber diameter and polymeric concentrations. Higher polymeric concentrations, results thicker fiber diameters due to the large number of chain entanglements resulting less mobility of molecules minimizing the stretching of fibers during the spinning. However, it seems that there is not a direct correlation with fiber density. Due to the differences in fiber density significantly affects the values of contact angle. Higher densities produce more overlapping of fibers creating more pores eventually becomes filled by the air.

5.2 Contact Angle of Nonwoven Polymeric Nanofiber Mats

High polymeric concentrations result broader fiber distributions and thicker fiber diameters. The values of GSM (grams per square meter) demonstrates the fiber density, larger values of GSM increase the amount of fibers decreasing porosity and the number of pores. However, as fiber diameter increases, it decreases the size of the pores reducing the amount of air at the surface. Figure 16 shows a 3-Dimensional random distribution of nonwoven mats, it

provides an idea of the development of pores at the surface due to the random direction of fibers. It also helps to visualize the relation of GSM value with the overlapping of fibers at the surface.

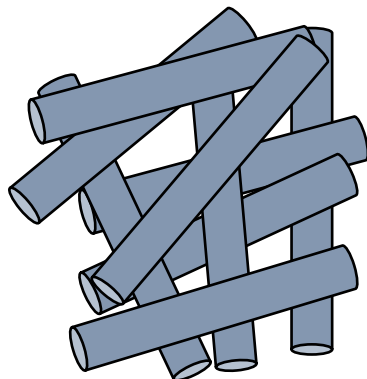


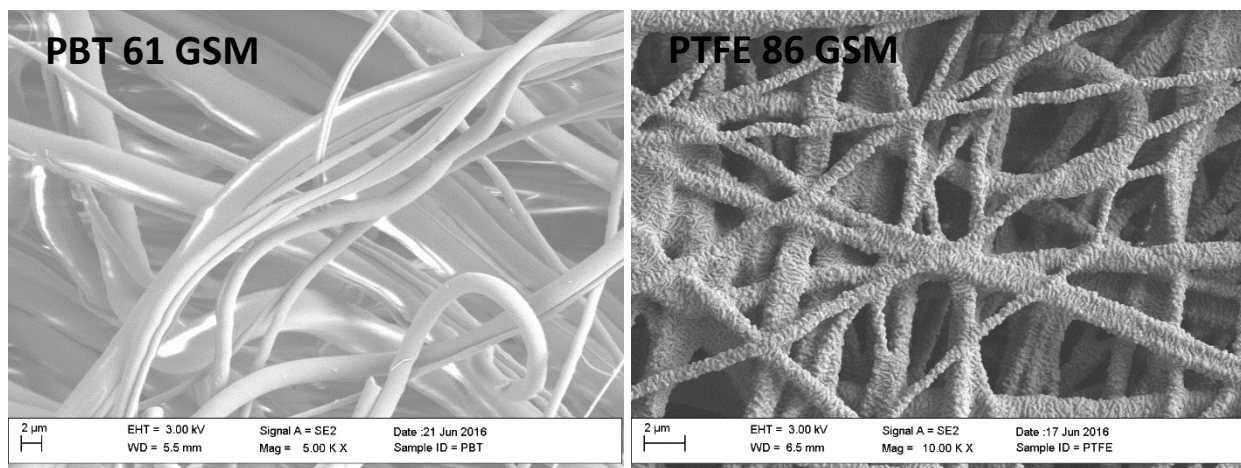
Figure 16. 3D Random distribution nonwoven mat

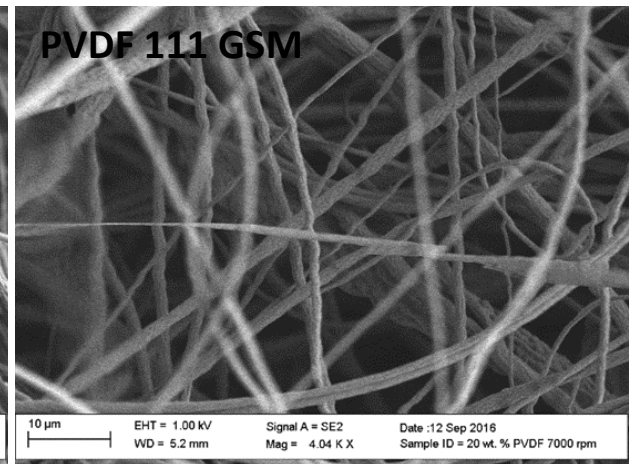
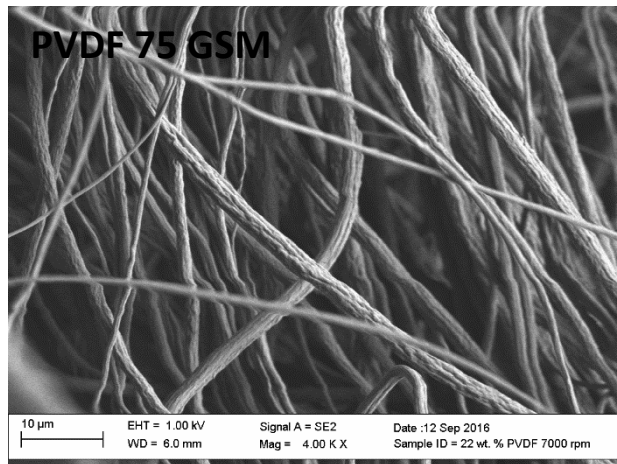
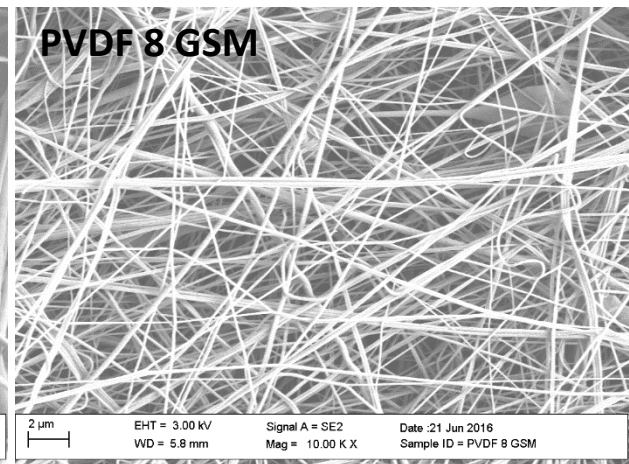
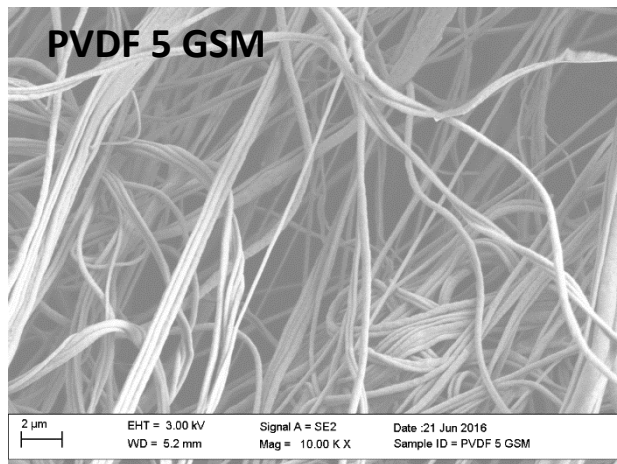
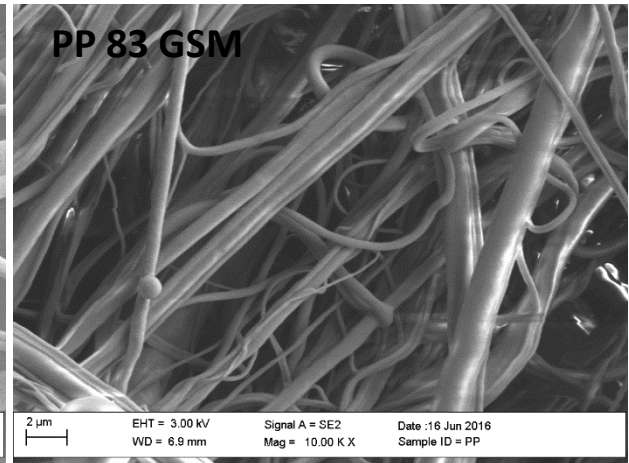
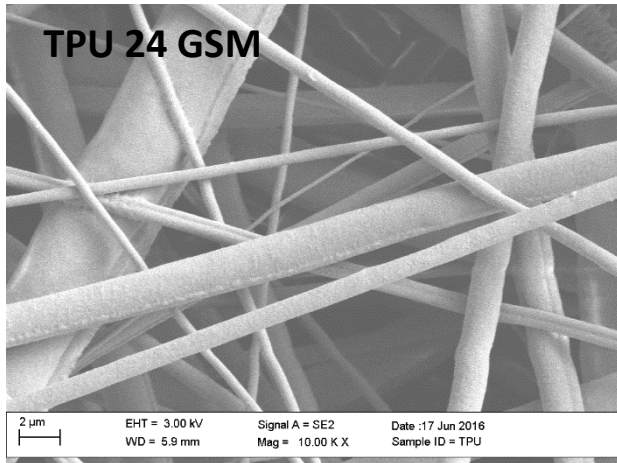
It is clearly seen by the represented morphology on the image that fiber density is higher on PVDF 8 GSM. Table 3 demonstrates the analysis conducted on PVDF fiber mats, it shows the contact angles of bulk and fiber mats at 5 and 8 GSM resulted values of 0.44 and 0.23 μm and contact angle values of 152.17° and 175.25° , respectively. Even though an increasing trend in contact angle is expected as GSM increases, it is to be noted that one should pay attention to the fiber diameter as well since pore size will be also strongly dependent upon fiber diameter. The sample that shows the higher contact angles was the 8 GSM system. The trend is followed by the 5 GSM sample and then a significant drop in contact angle is observed for the others systems which shown much larger fiber diameters. The highest value of contact angle due to higher fiber density results a higher number of fibers overlapped producing a larger number of pores filled with air, resulting high contact angle values. However, in the case of PVDF 20wt.% (111 GSM), 22wt.% (75 GSM) and 24wt.% (114 GSM), with contact angle values of 125.68° , 118.90° and 128.59° , respectively. Exists a strong correlation between contact angle and GSM values. All three different nanofiber mats were forcespun at a constant rotational speed of 7000 rpm. 24wt.% (114

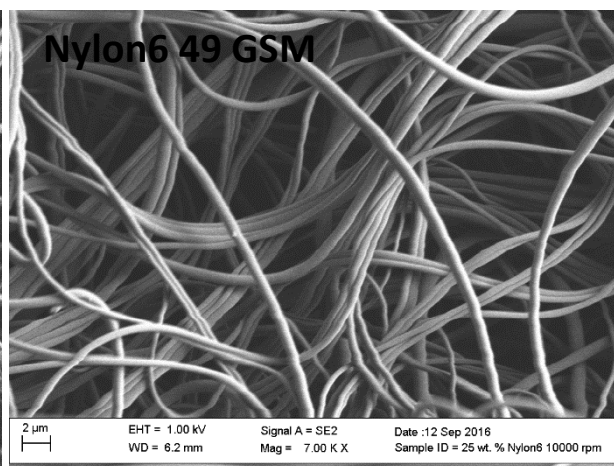
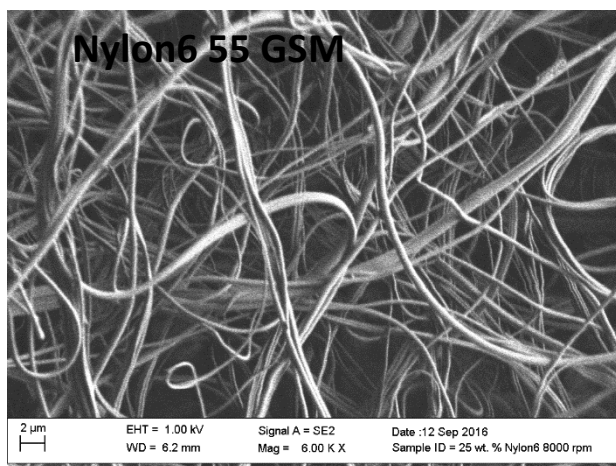
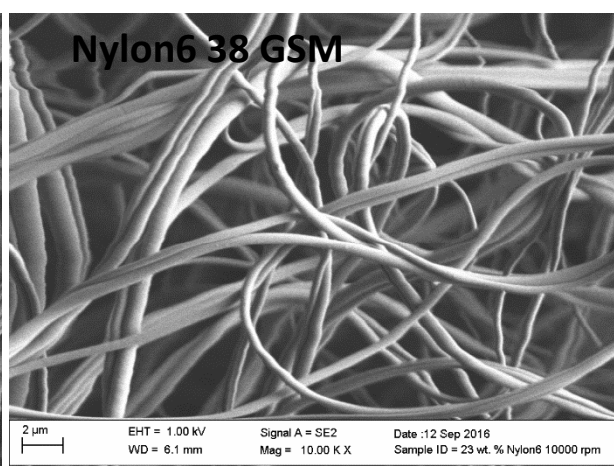
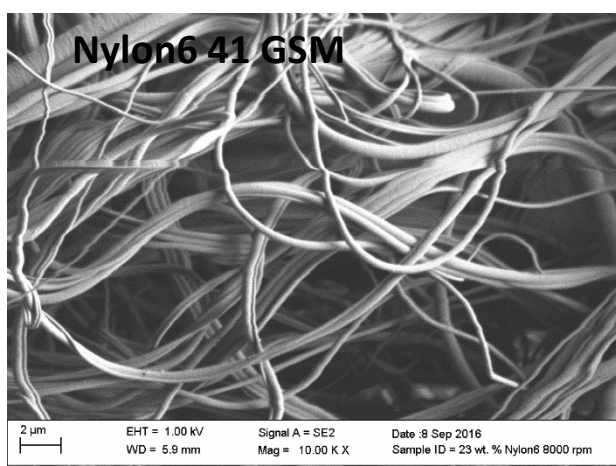
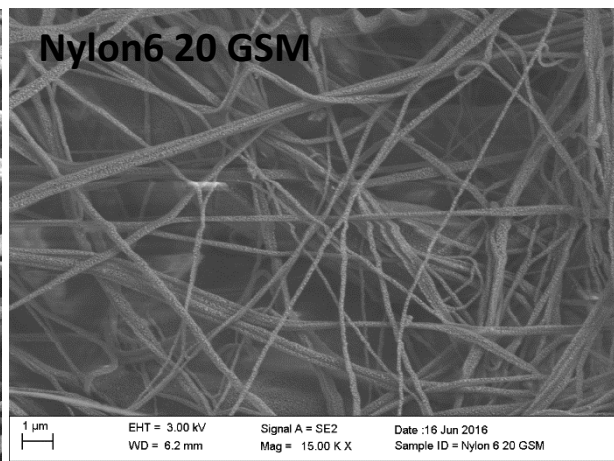
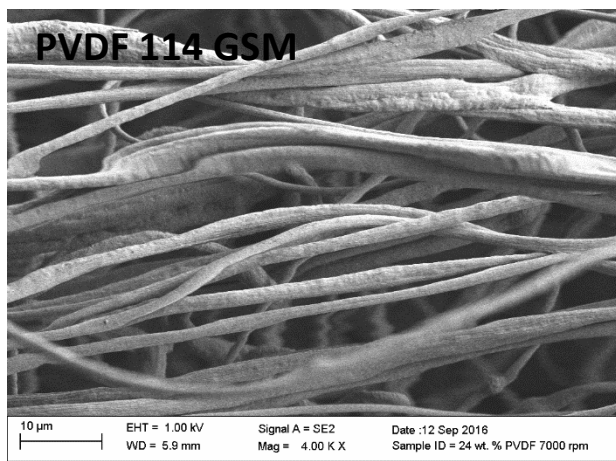
GSM) shows the highest contact angle value of 128.59° due to the development of smaller pores due to the large number of fibers overlapped on the surface.

Higher concentrations of fibers at the surface results smaller pore sizes, increasing the amount of air at the surface. Larger concentrations of air results higher contact angles due amount of forces against the weight of the droplet produced by the air.

Table 2, demonstrates the contact angles for Nylon6 fiber mats at different GSM's. Nylon6 is a hygroscopic material that absorbs water. When water is in contact with the surface, it forms a capillary film between the pores holding the water droplet on the surface developing hydrophilic contact angles. However, it still exists an interrelation between fiber diameters and contact angle values. Nylon6 72 GSM demonstrates the highest angle value of 117.99° due to number of fibers at the surface developing small size pores compared to the other GSM values. In the case of Nylon6 20 GSM with the smallest fiber diameter of $0.14\text{ }\mu\text{m}$, demonstrates a contact angle of 95.83° due to the lower fiber density.







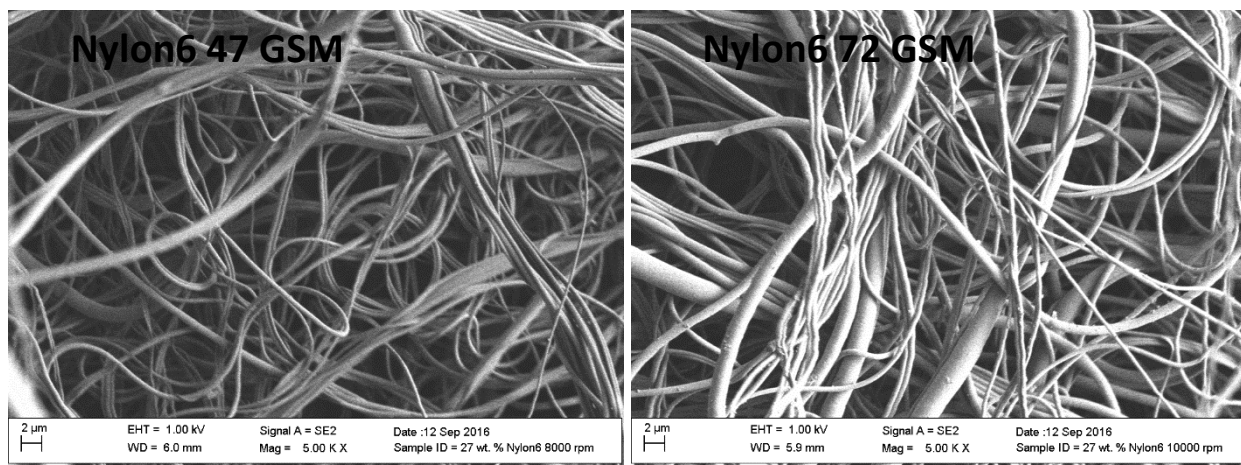


Figure 17. SEM Images of various fiber mats fabricated by Forcespinning

Table 2. Contact angles and Work of adhesion of Bulk and Fibers for Nylon6

Nylon6					
	Bulk		Fiber		
	Contact Angle (°)	Work of Adhesion (mJ/m ²)	Contact Angle (°)	Work of Adhesion (mJ/m ²)	Fiber Diameter (μm)
20 GSM	58.69	109.75	95.83	84.80	0.14
38 GSM	58.69	109.75	87.66	87.66	0.75
41 GSM	58.69	109.75	94.95	66.53	0.47
47 GSM	58.69	109.75	102.38	75.40	0.63
49 GSM	58.69	109.75	90.72	71.88	0.64
55 GSM	58.69	109.75	91.40	71.00	0.54
72 GSM	58.69	109.75	117.99	73.74	0.66

5.3 Work of Adhesion of Nonwoven Polymeric Nanofiber Mats

Work of adhesion represents the strength of contact between the two adjacent phases. It describes the strength of the interface defining the work needed to separate the interface. It is important to obtain a general approach of the forces at the molecular level acting during the contact between two phases. Table 2 demonstrates the values of work of adhesion of Nylon6 nanofiber mats. Exists an opposite relation between the values of GSM and work of adhesion. High fiber densities increase the number of pores resulting higher concentrations of air producing high values of contact angle. 38 GSM shows the higher fiber diameter demonstrating the highest value of work

of adhesion 87.66 mJ/m^2 . Thicker fiber diameters usually decrease the pore size and air content at the surface resulting a strong contact with the surface requiring more energy to detach the solid and liquid phase.

Table 3, demonstrates the contact angles of bulk and fiber forms for PVDF materials at different GSM's. In the case of PVDF truly demonstrates the porosity formed by the fiber diameter. 8 GSM showed smallest fiber diameter with a contact angle of 175.25° with a value of 69.68 mJ/m^2 . Due to the low value of GSM the pores are still larger providing enough room for the water to move further down taking more energy to remove it. 5 GSM the second smaller diameter the contact angle is still high; even though, the diameter is still thicker than 8 GSM pores are still smaller that water still stays on the surface with a work of adhesion of 32.01 mJ/m^2 . However, PVDF 114 GSM showed the lowest value of work of adhesion of 27.45 mJ/m^2 , even though has the largest fiber diameter value, due to the higher fiber density creating larger number of pores. In the case of 75 and 111 demonstrated 44.64 mJ/m^2 , 47.58 mJ/m^2 , respectively almost the same. It might be due to their almost identical value of fiber diameter. Even though 111 GSM is creating a lot more pores than 75 GSM, since the fiber diameter are almost the same thickness the pore sizes are almost the same.

Table 4, demonstrates contact angles and work of adhesion for fiber and bulk surfaces for various polymers. Based on the information in the table PTFE followed by TPU demonstrated contact angles of 175.43° and 171.19° , respectively. However, PTFE demonstrated lower work of adhesion than TPU. Due to the morphology of PTFE as shown in Figure 14 (B) where a, hierarchical pattern is observed which increases the surface area.

Table 3. Contact angles and Work of adhesion of Bulk and Fiber mats for PVDF.

PVDF					
	Bulk		Fiber		
	Contact Angle (°)	Work of Adhesion (mJ/m ²)	Contact Angle (°)	Work of Adhesion (mJ/m ²)	Fiber Diameter (μm)
5 GSM	97.95	109.19	152.17	32.01	0.44
8 GSM	97.95	109.19	175.25	69.68	0.23
75 GSM	97.95	109.19	118.90	44.64	1.74
111 GSM	97.95	109.19	125.68	47.58	1.73
114 GSM	97.95	109.19	128.59	27.45	1.81

Table 4. Contact angles and Work of adhesion for Bulk and Fiber mats for Various Polymer.

Various Polymers					
	Bulk		Fiber		
	Contact Angle (°)	Work of Adhesion (mJ/m ²)	Contact Angle (°)	Work of Adhesion (mJ/m ²)	Fiber Diameter (μm)
PP 83 GSM	103.53	55.8	115.87	31.94	0.58
PBT 61 GSM	78.66	86.91	168.85	38.69	2.14
TPU 24 GSM	79.59	85.85	171.19	34.60	1.49
PTFE 86 GSM	125.68	30.60	175.43	30.6	0.99

In the case of heterogeneous surface, which is the case of nonwoven nanofiber mats the weight is concentrated on the sidewalls of fibers. The penetration of the droplet is restricted due to a considerable decrease of fraction of fibers in contact with the liquid. As shown in Figure 18, due to the restricted space of the fibers, the droplet forms a sag that could eventually be in contact with the bottom surface. Fibers are randomly oriented, not regularly spaced in a nonwoven mat distributed in a non-stochastic orientation [48]. It is important to understand that the roughness of the forcespun nonwoven nanofiber mats is caused by the regions covered by the overlapping fibers, dramatically decreasing the surface contact area of the droplet with the mat therefore, developing a discontinuous three-phase contact exhibiting superhydrophobicity.

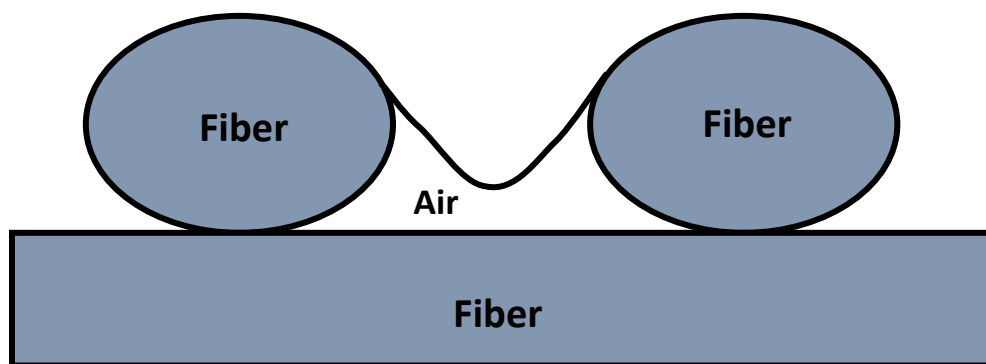


Figure 18. Schematic Illustrating the sagging of liquid on the fiber surface.

The sagging of the interface is strongly affected by the increase in the air pockets. Similarly, the force applied by the weight of the droplet develops a pressure on the surface. Higher magnitude of pressure under the droplet indicates that more time is required to wet the forcespun nanofiber mat. However, the pressure differences at the interface can significantly increase by reducing the fiber diameter. In Addition, the overlapping areas of fibers are responsible for developing a roughness in the nonwoven nanofiber mat that produces an influence in the wettability and mechanical properties. The forcespun nonwoven can be engineered for superhydrophobicity properties by enhancing the fiber diameter and GSM resulting an influence on the roughness.

CHAPTER VI

CONCLUSION

The wettability of nonwoven mats was analyzed for a variety of polymeric systems. Fiber diameter and aerial density were varied and its influence on contact angles and work of adhesion was evaluated. It was observed that for systems where the fiber diameter is in the nanoscale, the Cassie Baxter mechanism was responsible for the observed superhydrophobic behavior. Surface roughness of the fibers also contributed to the increase in contact angle values. The systematic study provides knowledge to further develop important applications such as self-cleaning systems, anti-fouling membranes, and battery separators such as polymer electrolyte and rechargeable batteries.

CHAPTER VII

FUTURE APPLICATIONS

The superhydrophobic behavior of nonwoven systems offer an unparalleled opportunity to the filtration, smart coatings (anti-fouling) and textile industries. Superhydrophobicity is a character that is been increasingly in the performance of technical textiles such as clothing and home textiles. Superhydrophobicity plays an important role to attain effectively liquid repellence, self-cleaning, including functionalities such as bacterial, stain resistant, and UV protection, surface functionalities, and high mechanical performance. Those are some of the applications where nonwoven nanofiber mats can be implemented due to their characteristics. Microfluidics, water harvesting systems, are applications where nanofiber mats are being evaluated and understood their characteristics to manipulate the direction of the flow of a fluid related to hydrophilicity in microfluidics. And the wettability of fibers to trap water molecules from the environment and collected them for future usage in harvesting systems. Those are experienced systems of applications.

However, the evaluation of Algal attachment to nanofiber mats and air filtration could be potential studies that provides a better understanding of attachment of the marine algae to nanofiber mats, and the pressure drop produced by the pore size interrelated to fiber diameter, respectively. The approach to assess the antifouling property of nonwoven nanofiber mats is by exposing mat samples to growing algal culture identifying the nanofiber mat the best prohibits the adherence of algae to its surface. The attachment of algae is particularly related to the biofilm that

consists of a group of bacteria, algae, fungi, and protozoans. Fiber diameter is an important parameter that determines the efficiency of filtration systems due to the pressure drop generated by pore size. Filtration efficiency is associated to the fiber thickness; the pore elements of filters must be at scale of the particles to be captured. Due to the high surface area, tiny particles of $<0.5\ \mu\text{m}$ can be easily trapped in the nonwoven nanofiber mats. Studying a variety of fiber diameters and pore sizes calculating the pressure drop based on the airflow in and out of the nonwoven nanofiber mat, an optimum pore size and fiber diameter can be determined.

REFERENCES

1. Zhang L, Zhang X, Dai Z, Wu J, Zhao N, Xu J. Micro-nano hierarchically structured nylon 6,6 surfaces with unique wettability. *J Colloid Interface Sci.* 2010;345(1):116–9.
2. Anantharaju N, Panchagnula M V., Vedantam S. Asymmetric wetting of patterned surfaces composed of intrinsically hysteretic materials. *Langmuir.* 2009;25(13):7410–5.
3. Yang WJ, Neoh K-G, Kang E-T, Teo SL-M, Rittschof D. Polymer brush coatings for combating marine biofouling. *Prog Polym Sci.* 2014;39(5):1017–42.
4. Carson RT, Damon M, Johnson LT, Gonzalez J a. Conceptual issues in designing a policy to phase out metal-based antifouling paints on recreational boats in San Diego Bay. *J Environ Manage.* 2009;90(8):2460–8.
5. Chambers LD, Stokes KR, Walsh FC, Wood RJK. Modern approaches to marine antifouling coatings. *Surf Coatings Technol.* 2006;201(6):3642–52.
6. Arukalam IO, Oguzie EE, Li Y. Fabrication of FDTD-modified PDMS-ZnO nanocomposite hydrophobic coating with anti-fouling capability for corrosion protection of Q235 steel. *J Colloid Interface Sci.* 2016;484:220–8.
7. Jiang S, Cao Z. Ultralow-Fouling, Functionalizable, and Hydrolyzable Zwitterionic Materials and Their Derivatives for Biological Applications. *Adv Mater.* 2010;22(9):920–32.
8. Teli SB, Molina S, Calvo EG, Lozano AE, de Abajo J. Preparation, characterization and antifouling property of polyethersulfone–PANI/PMA ultrafiltration membranes. *Desalination.* 2012;299:113–22.
9. Heyer A, D’Souza F, Morales CFL, Ferrari G, Mol JMC, de Wit JHW. Ship ballast tanks a review from microbial corrosion and electrochemical point of view. *Ocean Eng.* 2013;70:188–200.
10. Schultz MP, Bendick JA, Holm ER, Hertel WM. Economic impact of biofouling on a naval surface ship. *Biofouling.* 2011;27(1):87–98.
11. Kim P, Wong T-S, Alvarenga J, Kreder MJ, Adorno-martinez WE, Aizenberg J, et al.

Liquid-Infused Nanostructured Surfaces with Extreme Anti-Ice and Anti-Frost Performance. *ACS Nano*. 2012;6(8):6569–77.

12. Strobl T, Storm S, Kolb M, Haag J, Hornung M. Development of a Hybrid Ice Protection System Based on Nanostructured Hydrophobic Surfaces. 2014;1–12.
13. Sarkar DK, Farzaneh M. Superhydrophobic Coatings with Reduced Ice Adhesion. *J Adhes Sci Technol*. 2009;23(9):1215–37.
14. Kulinich SA, Farhadi S, Nose K, Du XW. Superhydrophobic surfaces: Are they really ice-repellent? *Langmuir*. 2011;27(1):25–9.
15. Zou M, Beckford S, Wei R, Ellis C, Hatton G, Miller MA. Effects of surface roughness and energy on ice adhesion strength. *Appl Surf Sci*. 2011;257(8):3786–92.
16. M N, Mechanics EM. is satisfied locally at the triple line a liquid front spreads along a flat solid surface, the net free surface energy (per front length) is given by $W(\gamma)$. *Society*. 2007;1(4):9919–20.
17. Bracco G, Holst B. Surface science techniques. Vol. 51, Springer Series in Surface Sciences. 2013.
18. Yildirim Erbil H, Elif Cansoy C. Range of applicability of the wenzel and cassie-baxter equations for superhydrophobic surfaces. *Langmuir*. 2009;25(24):14135–45.
19. Cansoy CE, Erbil HY, Akar O, Akin T. Effect of pattern size and geometry on the use of Cassie-Baxter equation for superhydrophobic surfaces. *Colloids Surfaces A Physicochem Eng Asp*. 2011;386(1–3):116–24.
20. Lin J, Cai Y, Wang X, Ding B, Yu J, Wang M. Fabrication of biomimetic superhydrophobic surfaces inspired by lotus leaf and silver ragwort leaf. *Nanoscale*. 2011;3(3):1258–62.
21. Liu K, Jiang L. Bio-Inspired Self-Cleaning Surfaces. 2012;231–65.
22. Ozbay S, Erbil HY. Ice accretion by spraying supercooled droplets is not dependent on wettability and surface free energy of substrates. *Colloids Surfaces A Physicochem Eng Asp*. 2016;504:210–8.
23. Joshi MK, Tiwari AP, Maharjan B, Won KS, Kim HJ, Park CH, et al. Cellulose reinforced nylon-6 nanofibrous membrane: Fabrication strategies, physicochemical characterizations, wicking properties and biomimetic mineralization. *Carbohydr Polym*. 2016;147:104–13.
24. Huang FL, Wang QQ, Wei QF, Gao WD, Shou HY, Jiang SD. Dynamic wettability and contact angles of poly(vinylidene fluoride) nanofiber membranes grafted with

acrylic acid. *Express Polym Lett.* 2010;4(9):551–8.

25. Buga M-R, Zaharia C, Bălan M, Bressy C, Ziarelli F, Margailan A. Surface modification of silk fibroin fibers with poly(methyl methacrylate) and poly(tributylsilyl methacrylate) via RAFT polymerization for marine antifouling applications. *Mater Sci Eng C.* 2015;51:233–41.
26. Xie Y, Hill CAS, Xiao Z, Militz H, Mai C. Silane coupling agents used for natural fiber/polymer composites: A review. *Compos Part A Appl Sci Manuf.* 2010;41(7):806–19.
27. Hermanson GT. Silane Coupling Agents. *Bioconjugate Tech.* 2013;535–48.
28. Jhaveri JH, Murthy ZVP. A comprehensive review on anti-fouling nanocomposite membranes for pressure driven membrane separation processes. *Desalination.* 2016;379:137–54.
29. Zhang Q, Zhang S, Dai L, Chen X. Novel zwitterionic poly(arylene ether sulfone)s as antifouling membrane material. *J Memb Sci.* 2010;349(1–2):217–24.
30. Pereira VR, Isloor AM, Bhat UK, Ismail AF. Preparation and antifouling properties of PVDF ultrafiltration membranes with polyaniline (PANI) nanofibers and hydrolysed PSMA (H-PSMA) as additives. *Desalination.* 2014;351:220–7.
31. Akbari A, Aliyarizadeh E, Mojallali Rostami SM, Homayoonfal M. Novel sulfonated polyamide thin-film composite nanofiltration membranes with improved water flux and anti-fouling properties. *Desalination.* 2016;377:11–22.
32. Rana D, Matsuura T. Surface modifications for antifouling membranes. *Chem Rev.* 2010;110(4):2448–71.
33. Zhao X, Su Y, Li Y, Zhang R, Zhao J, Jiang Z. Engineering amphiphilic membrane surfaces based on PEO and PDMS segments for improved antifouling performances. *J Memb Sci.* 2014;450:111–23.
34. Lundin JG, Coneski PN, Fulmer P a., Wynne JH. Relationship between surface concentration of amphiphilic quaternary ammonium biocides in electrospun polymer fibers and biocidal activity. *React Funct Polym.* 2014;77:39–46.
35. Dasari A, Quiros J, Herrero B, Boltes K, Garcia-Calvo E, Rosal R. Antifouling membranes prepared by electrospinning polylactic acid containing biocidal nanoparticles. *J Memb Sci.* 2012;405–406:134–40.
36. Shi H, Liu H, Luan S, Shi D, Yan S, Liu C, et al. Antibacterial and biocompatible properties of polyurethane nanofiber composites with integrated antifouling and bactericidal components. *Compos Sci Technol.* 2016;127:28–35.

37. Louie JS, Pinnau I, Ciobanu I, Ishida KP, Ng A, Reinhard M. Effects of polyether–polyamide block copolymer coating on performance and fouling of reverse osmosis membranes. *J Memb Sci*. 2006;280(1–2):762–70.
38. Manuscript A, Morphology C. NIH Public Access. *Macromolecules*. 2008;40(17):6283–90.
39. Abdal-Hay A, Pant HR, Lim JK. Super-hydrophilic electrospun nylon-6/hydroxyapatite membrane for bone tissue engineering. *Eur Polym J*. 2013;49(6):1314–21.
40. Abdal-Hay A, Hamdy AS, Khalil KA. Fabrication of durable high performance hybrid nanofiber scaffolds for bone tissue regeneration using a novel, simple in situ deposition approach of polyvinyl alcohol on electrospun nylon 6 nanofibers. *Mater Lett*. 2015;147:25–8.
41. Sekhon S. Ionic conductivity of PVdF-based polymer gel electrolytes. *Solid State Ionics*. 2002;152–153:169–74.
42. Obregon N, Agubra V, Pokhrel M, Campos H, Flores D, De la Garza D, et al. Effect of Polymer Concentration, Rotational Speed, and Solvent Mixture on Fiber Formation Using Forcespinning®. *Fibers*. 2016;4(2):20.
43. Megelski S, Stephens JS, Bruce Chase D, Rabolt JF. Micro- and nanostructured surface morphology on electrospun polymer fibers. *Macromolecules*. 2002;35(22):8456–66.
44. Sarkar K, Gomez C, Zambrano S, Ramirez M, Hoyos E De, Vasquez H, et al. Electrospinning to. 2010;13(11):13–5.
45. Stalder AF, Melchior T, Müller M, Sage D, Blu T, Unser M. Low-bond axisymmetric drop shape analysis for surface tension and contact angle measurements of sessile drops. *Colloids Surfaces A Physicochem Eng Asp*. 2010;364(1–3):72–81.
46. Gao L, McCarthy TJ. Ionic liquids are useful contact angle probe fluids. *J Am Chem Soc*. 2007;129(13):3804–5.
47. Ryu YJ, Kim HY, Lee KH, Park HC, Lee DR. Transport properties of electrospun nylon 6 nonwoven mats. *Eur Polym J*. 2003;39(9):1883–9.
48. Rawal A. Design parameters for a robust superhydrophobic electrospun nonwoven mat. *Langmuir*. 2012;28(6):3285–9.

BIOGRAPHICAL SKETCH

EDGAR MUNOZ, currently residing at 2906 De La Rosa Dr. Donna, TX. Obtained his Master of Science in Mechanical Engineering (MSME) – Materials Track from the University of Texas Rio Grande Valley in December 2016. Throughout his graduate education, developed an interest of education and commitment with science and engineering. Edgar Muñoz obtained his Bachelor of Science in Mechanical Engineering (BSME) from the University of Texas Pan-American in May 2014. Joining one of the largest service company in the energy workforce after obtaining his BSME. He started working at a younger age in service organizations including food and oil industries having the opportunity of learning working in teams developing interpersonal skills, respect for others building a strong attitude of helping others. Throughout his professional and academic career, Mr. Muñoz had understood the importance of collaborating with other and working hard to accomplish goals and dreams.